FUNCTIONAL AND STRUCTURAL ANALYSIS OF THE MOUSE ATPASE II GENE

by

Farah A. Jayman

A dissertation submitted to the Graduate Faculty in Biochemistry in partial fulfillment of the requirements for the degree of

Doctor of Philosophy

The City University of New York

2006

UMI Number: 3213256

ProQuest Information and Learning Company
300 North Zeeb Road
P.O. Box 1346
Ann Arbor, MI 48106-1346

This manuscript has been read and accepted by the Graduate Faculty in Biochemistry in satisfaction of the dissertation requirements for the degree of Doctor of Philosophy

_____	_____
Date	Chairperson of Examining Committee Dr. Probal Banerjee
_____	_____
Date	Executive Officer Dr. Lesley Davenport

Dr. Andrzej Wieraszko, The College of Staten Island, CUNY

Dr. Raju Pullarkat, Institute for Basic Research, CUNY

Dr. Chang-Hui Shen, The College of Staten Island, CUNY

Dr. David Calhoun, City College, CUNY

Supervisory Committee

THE CITY UNIVERSITY OF NEW YORK

THE CITY UNIVERSITY OF NEW YORK

ABSTRACT

FUNCTIONAL AND STRUCTURAL ANALYSIS
OF
THE MOUSE ATPASE II GENE

by

Farah Jayman

Advisor: Professor Probal Banerjee

Normally, PS is located in the inner leaflet of the plasma membrane, however during apoptosis externalization of PS to the outer leaflet of apoptotic cells induces macrophages containing surface PS receptors to engulf these cells. In healthy cells a bifunctional enzyme, which is a Mg^{2+}-ATPase, as well as an aminophospholipid translocase (APTL), is responsible for the translocation of PS from the outer leaflet of the plasma membrane to the inner. Phospholipid asymmetry is relatively stable and is believed to be maintained by the enzymes APTL, Scramblase (which bidirectionally translocates all phospholipids) and floppase (which slowly translocates phospholipids from the inner leaflet to the outer).ATPase II is a Mg^{2+}-ATPase II that is also a good candidate for the enzyme aminophospholipid translocase (APTL). The main objective of this project is to provide evidence for the hypothesis that ATPase II is indeed an APTL. In doing so, we have shown that the overexpression of the mouse *ATPase II* cDNA in mouse neuroblastoma cells causes increased PS translocation, inhibition of caspase-3, and also activation of Erk 1/2, which regulates gene expression and apoptosis. We also expressed antisense, full-length ATPase II cDNA, which showed externalization of PS and the inhibition of its APTL activity in healthy cells. This observation shows us that

ATPase II could indeed have an APTL like activity or could be involved in regulating the APTL activity. Additionally, our results indicate that ATPase II could also have signaling activity. Previous studies have shown that the expression of ATPase II mRNA is tissue-specific, with the highest level of expression seen in brain and skeletal muscle. In order to study the mechanism of cell type-specific expression of ATPase II, the 5' upstream sequence of the mouse *ATPase II* gene has been isolated. A 1.5-kb 5' flanking sequence of this gene bears considerable homology to and some significant differences from the human *ATPase II* promoter that has been isolated and analyzed. The transcription start site and regulatory elements have been analyzed using 5'-RACE and deletion analysis of the putative mouse *ATPase II* promoter. Results from RACE and promoter activity studies show that there is some cell type specific activity of this ATPase promoter. It has been shown by many groups including ours that macrophages (microglia in the brain) recognize phosphatidylserine (PS) when it is exposed on the cell surface. Therefore, a strategy of down regulating ATPase II could be used to trigger the engulfment of unwanted cells via recognition of externalized PS by the PS receptors present on scavenger cells.

I dedicate this thesis to my loving family: To Dadda and Mummy for all what you gave up to give us an education and a better life. And to my sisters Razia and Shireen, you all jointly made it possible for me to complete my thesis and come this far in life.
With out all of you I am not complete.

ACKNOWLEDGEMENTS

This work could not be brought to a thesis stopping point without the efforts of hardworking and dedicated people. The author wishes to express deep gratitude to all the members of the Chemistry department of the College of Staten Island and Biochemistry doctoral program at the Graduate School of the City University of New York for all the moral and financial support. This project was supported and funded by the Alliance for Graduate Education and the Professoriate (AGEP) program, the Alliance for Minority Participation (AMP) program of the City University of New York, the National Insititute of Health (NIH) minority supplement and my parents. A special thanks and appreciation goes to the ever so patient and encouraging mentor of this project Dr. Probal Banerjee for his scientific wisdom, efforts in helping direct the project, and the endless advise both personal and academic. Additionally to the members of the supervisory committee thank you from the bottom of my heart for your guidance, helpful discussions and input. Also the members of Dr. Banerjee's lab: A special thanks to Margaret and Tomasz for your insights and guidance with the project. Sincere thanks to Tanya for passing her wisdom and knowledge on. I would also like to thank my dearest friends and lab partners Baishali, Kelly, Shawn and Mukti for all your support and the shoulders provided to lean on – you all are true friends indeed.

Finally, I would like to thank my immediate family members who were and are very supportive, understanding and patient in helping finish my thesis. A special thank you to my sisters, especially Shireen for putting up with my mood swings during those down days. Last but not least, thank you to my loving husband Azkar for bringing happiness into my life, you made it easy for me to get to the finish line.

Table of Contents

List of Tables and Figures

ABBREVIATIONS

AIF	Apoptosis Initiating Factors
Apaf-1	Apoptotic Protease-Activating factor 1
Apo-1	Apoptosis-inducing or death receptors
Bcl-2	B-cell leukemia/lymphoma 2
BSA	bovine serum albumin
CPP-32	Caspase-3, casp-3, Yama
Ca	Calcium
DMEM	Dulbecco's modified Eagle's medium
ERK 1/2	extracellular signal regulated kinase 1/2 , MAPK
FBS	fetal bovine serum
GFP	green fluorescence protein
H_2O_2	hydrogen peroxide
HBS	Hepes buffered saline
HRP	horse-reddish peroxydase
IGF-1	insulin-like growth factor-1
KRB	Krebs-Ringers buffer
NBD-PS	1-Oleoyl-2-C6-[7-nitro-2-oxa-1,3-diazol-4-ylamino] caproy1-sn-glycero-3-phosphoserine
PAGE	polyacrylamide gel electrophoresis
PBS	phosphate-buffered saline
PMSF	phenylmethylsulfonyl fluoride
PS	phosphatidylserine

PS	penicillin-streptomycin
RIPA	radioimmune precipitation buffer
SDS	sodium dodecyl sulfate
TBS	tris-buffered saline
TBST	Tris-buffered saline + Tween 20
VDCC	Voltage Dependent Calcium Channels

Chapter 1

Introduction:

Apoptosis:

The occurrence of cell death during normal development of multicellular organisms had been observed and commented upon as early as in the nineteenth century [Review, Becker 2004]. The term "programmed cell death" was used to describe metamorphosing insect muscle cells that undergo a sequence of controlled steps towards their own destruction [Review, Becker 2004]. This idea was later generalized by various researchers, who suggested that active and precisely controlled cell death serves as a homeostatic function in regulating the size of cell populations under both normal and pathophysiologic condictions [Review, Becker 2004]. Apoptosis (programmed cell death) is a highly conserved cellular process in eukaryotes that is comprised of a stereotyped sequence of biochemical and morphological changes. It is characterized biochemically by internucleosomal DNA fragmentation and morphologically by nuclear and cytoplasmic condensation, along with membrane blebbing [Zwaal, 1997]. Little damage occurs to the cell organelles in the initial stages of apoptosis. However, during necrotic (passive pathologic event, killing of the cell – arising from spontaneous insults, such as stroke or trauma) cell death, the dying cell and its contents swell and subsequently lyse, thereby provoking an inflammatory response. The absence of cell lysis in apoptosis allows the affected cell to die without adversely affecting its neighbors. A characteristic final step in apoptosis is the fragmentation of the cell into apoptotic bodies, which are subsequently phagocytosed by surrounding scavenger cells. Apoptosis plays an important role in cell removal during embryogenesis, morphogenesis, normal cell turnover, resolution of

hyperplasia and neoplasia [Zwaal, 1997]. It is carried out by an intrinsic suicidal machinery of the cell and can be triggered by environmental stimuli including irradiation leading to DNA damage, oxidative stress, toxins, viruses, etc. A characteristic feature of apoptosis is that it is an active ATP-dependent biochemical process. Apoptotic cell death is regulated through transcriptional as well as post-translational mechanisms. Studies showing inhibition of RNA and protein synthesis blockage in neuronal cell death induced by trophic factor withdrawal, was the first evidence that neurons actively die [Review, Becker 2004]. The principal molecular players of apoptosis include: a number of apoptosis-inducing or death receptors (e.g. Apo-1/Fas); Apaf-1 (apoptotic protease-activating factor 1) and other apoptosis-initiating factors (AIFs), small proteins released from damaged mitochondria into the cytoplasm in early stages of cell death; proteins/proteases of the caspase/calpain family; the Bcl-2 (B-cell leukemia/lymphoma 2) and p53 oncogene families; mitogen-activated protein kinase (MAPK) pathways regulated by neurotrophins. Once activated, many but not all of them induce proteolysis of specific cellular substructures and consequently amplify the death signal cascade. The central players of programmed cell death are the upstream initiator caspases (8,9, and 10), activating other caspases, named effector caspases (3, 6, and 7), important regulators of postmitotic neuronal homeostasis [Review, Becker 2004]. Such downstream caspases and their proteolytic products are recognized markers of apoptosis, their activation representing an irreversible step in the cell death cascade and cells expressing these enzymes are prone to death. The Bcl2 family includes a highly homologous group of mitochondrial proteins which act either to enhance (Bax, Bid, Bad, Bak, Bcl-x_S) or prevent (Bcl-2, Bcl-x_L) apoptosis by forming homo- or heterotypic dimers, which may

effect the formation of a permeability transition pore in the mitochondrial membranes [Review, Becker 2004] and the release of cytochrome c. Cytochrome c release from mitochondria into the cytoplasm leads to formation of a cytoplasmic complex of Apaf-1 and caspase 9, which results in caspase 9 activation. Subsequently caspase 9 cleaves and activates downstream caspase 3. Bcl-2 family members have also been suggested to elicit protective effects by preventing the release of Apaf-1/caspase-3 from the mitochondria.

Cysteine-dependent ASPartyl-specific proteASE (Caspases):

Virtually all animal cells contain caspases, but they occur as inactive zymogens than cannot do harm. There are various triggers that can lead to their activation, which usually occurs through proteolytic processing of the zymogen at conserved aspartic acid residues. Their activation and suicidal function is highly regulated. The name "caspase" denotes their function: Cysteine-dependent ASPartyl-specific proteASE. Caspases are protein-cleaving enzymes that fragment crucial proteins in a cell. The name refers to two properties of these enzymes. First, they are cysteine proteases that use the sulfur atom in cysteine to perform the cleavage reaction. Second, they cut proteins at the C-terminal end of residues such as aspartate. They do not cleave indiscriminately – instead, they are designed to make exactly the appropriate cuts needed to disassemble the cell in an orderly manner. Caspases are the major executioners of apoptosis. They act either as "initiator" proteases, whose activation characteristically sets in motion a caspase cascade, or as "effectors" (caspase 3, 6, 7) that degrade vital cellular proteins. Caspase targets include structural proteins such as the lamins and actin, DNA repair enzymes such as poly (ADP ribose) polymerase and topoisomerase I, and regulatory proteins such as the inhibitor of caspase activated DNase (ICAD). Once ICAD is cleaved off the caspase activated

DNase, this endonuclease cleaves the DNA into 180 base pair fragments, which results in the fragmentation of DNA, a known characteristic of apoptosis.

So far, upto 14 members of the caspase family have been identified, 11 of which are present in humans. Many of these proteases have been implicated in neuronal apoptosis. The first evidence that caspase activity is required for neuronal apoptosis came from experiments using pharmacological inhibitors of caspases. *Caspase-1, -2, -3, -9, -11,* and *-12* deficient mice show a neuronal phenotype, with *caspase -3* and *-9* deficient mice displaying the most severe defects in neuronal development [Review, Becker 2004]. In addition to developmentally regulated apoptosis, caspases may play pivotal roles in a number of neurologic disorders. For example, transgenic mice for a dominant negative mutant of caspase-1 has shown reduced sensitivity to ischemia as well as trophic factor deprivation [Review, Becker 2004].

Mitogen-activated protein kinases (MAPKs)

Mitogen activated protein kinases (MAPKs) are important signal trasnducing enzymes, unique to eurkaryotes, that are involved in many aspects of cellular regulation. MAPKs are evolutionarily conserved enzymes connecting cell-surface receptors to critical regulatory targets within cells. MAPKs also respond to chemical and physical stresses, thereby controlling survival and adaptation. Mammals express at least four distinctly regulated groups of MAPKs, extracellular signal related kinases (ERK) -1/2, Jun amino-terminal kinases (JNK 1/2/3), p38 proteins (p38 $\alpha/\beta/\gamma/\delta$), and ERK5, that are activated by specific MAPKKs [Chang 2001]. One of the most explored functions of MAPK signaling modules is regulation of gene expression in response to extracellular stimuli. JNKs phosphorylate Jun proteins, which subsequently enhance their ability to

activate transcription without affecting DNA binding. Most MAPKs phosphorylate transcription factors that are involved in induction of *fos* genes, whose products heterodimerize with Jun proteins to activation protein 1 (AP-1) complexes. In all cases, the MAPKs function inside the nucleus and target transcription factors that are pre-bound to DNA. Most transcription factors that are regulated by MAPKs are dimers, and structural analysis indicates that some MAPKs dimerize upon activation however, MAPK dimerization may fascilitate phosphorylation of dimeric transcription factors [Chang 2001]. MAPKs regulate cell proliferation. The ERKs can also stimulate cell proliferation indirectly by enhancing AP-1 activity, resulting in cyclin D1 induction. MAPKs also control cell survival. By and large, activation of ERK 1/2 has been linked to cell survival, whereas JNK and p38 are linked to induction of apoptosis. The actual role of each MAPK cascade are highly cell type and context dependent.

Phagocytosis and Membrane Assymetry

The uptake of apoptotic cells before they lyse suggests that a specific surface change occurs that is recognized by the phagocyte, however the mechanism of uptake is not clearly understood. As shown by Figure 1, it appears that the phagocytes taking up apoptotic cells may use one or more possible recognition mechanisms. There are three mechanisms for macrophage recognition of apoptotic cells, which have been described by other laboratories. Duvall *et al* suggested that a macrophage lectin bound to an abnormal or immature sugar group on the apoptotic thymocyte [Daleke 2000, Duvall 1985]. Savill *et al* showed that the macrophage vitronectin receptor bound to an unidentified negatively charged substance on the apoptotic neutrophil membrane [Fadeel 1999, Savill 1990]. Finally, it has been shown by many groups and our lab that macrophages (microglia in

the brain) recognize phosphatidylserine (PS) when it is exposed on the cell surface [Fadock 1992, Zwaal 1997]. Experiments reported by other labs, suggest that the removal of apoptotic cells does not depend on species-specific or tissue-specific surface markers. In fact, apoptotic cells may share common surface changes, one of which appears to be the exposure of PS on the external leaflet of the plasma membrane. Futhermore, the mechanism by which apoptotic cells are removed seems to be determined by the subpopulation of macrophages performing the function [Zwaal 1997]. The existence of multiple recognition mechanisms for the removal of apoptotic cells indicates the importance of this activity in maintaining normal tissue integrity.

The phospholipids of the animal cell plasma membrane are not randomly distributed across the bilayer; the aminophospholipids, PS and phosphatidylethanolamine (PE), are commonly present in the inner leaflet of the phospholipid bilayer. In contrast, the choline phospholipids, phosphatidylcholine (PC) and sphingomyelin, are present in the outer leaflet [Mouro 1999]. At least three distinct activities are involved in the regulation of membrane lipid asymmetry. Two energy-requiring activities seem to work together in maintaining a nonrandom transbilayer phospholipid orientation, as illustrated by Figure 2. Inhibition of these activities stops lipid movement, and restricts loss of asymmetry for at least several days in vitro [Tang 1996]. The loss of this asymmetry leads to the appearance of PS on the cell surface, which serves as a signal for phagocytosis of apoptotic lymphocytes and neurophils by macrophages [Halleck 1999]. Furthermore, the influx of Ca^{2+} into the cytoplasm, activates the enzyme scramblase, which causes rapid transbilayer phospholipid mixing that leads to a nearly symmetric distribution of phospholipids across the membrane bilayer [Mouro 1999].

The discovery of an ATP-dependent aminophospholipid translocase in red blood cells has provided direct evidence for the existence of mechanisms that generate and maintain membrane asymmetry through the transport of specific lipids across the cells membrane [Zwaal 1997]. This activity is distinguished by its ability to transport PS and PE (slower rate) from the outer leaflet of the plasma membrane to the inner. This process consumes one molecule of ATP per molecule of lipid (e.g. PS) transported. Transport is stereospecific for naturally occurring L-isomers of the glycerol-backbone and is inhibited by vanadate, sulfhydryl-reactive reagents *N*-ethylmaleimide and the histidine-reactive reagent bromophenacylbromide [Zwaal 1997]. In addition, activity is inhibited when cytosolic Ca^{2+} levels reach micromolar concentrations [Zwaal 1997]. These observations, clearly indicates that lipid transport is catalyzed by one or more membrane proteins, yet the identity of these proteins is still uncertain.

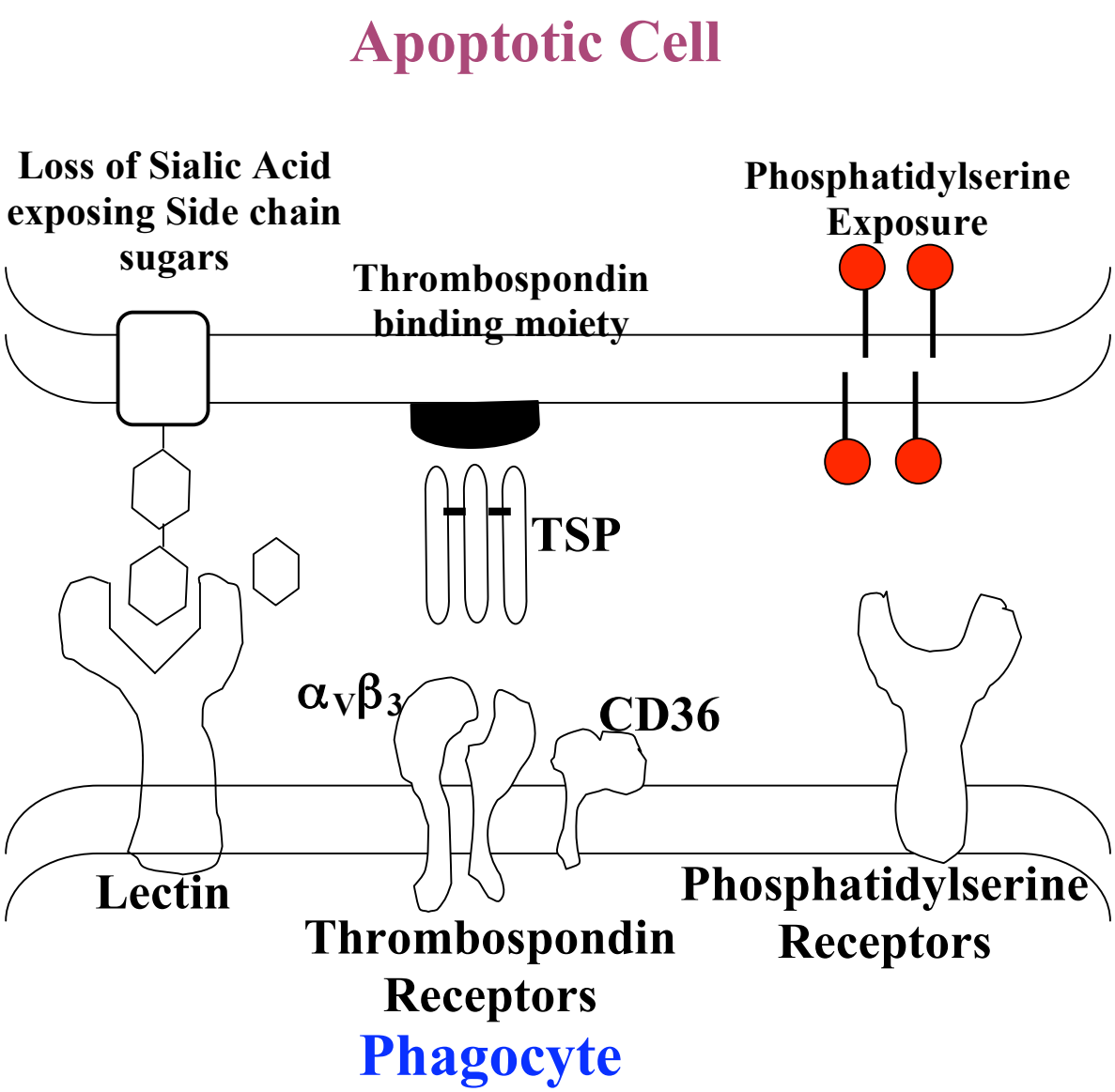

Figure 1: Three mechanisms by which phagocytes may recognize cells undergoing apoptosis. TSP – Thrombospondin. This figure is drawn using the figure from Duvall *et al* as a template [Duvall 1985].

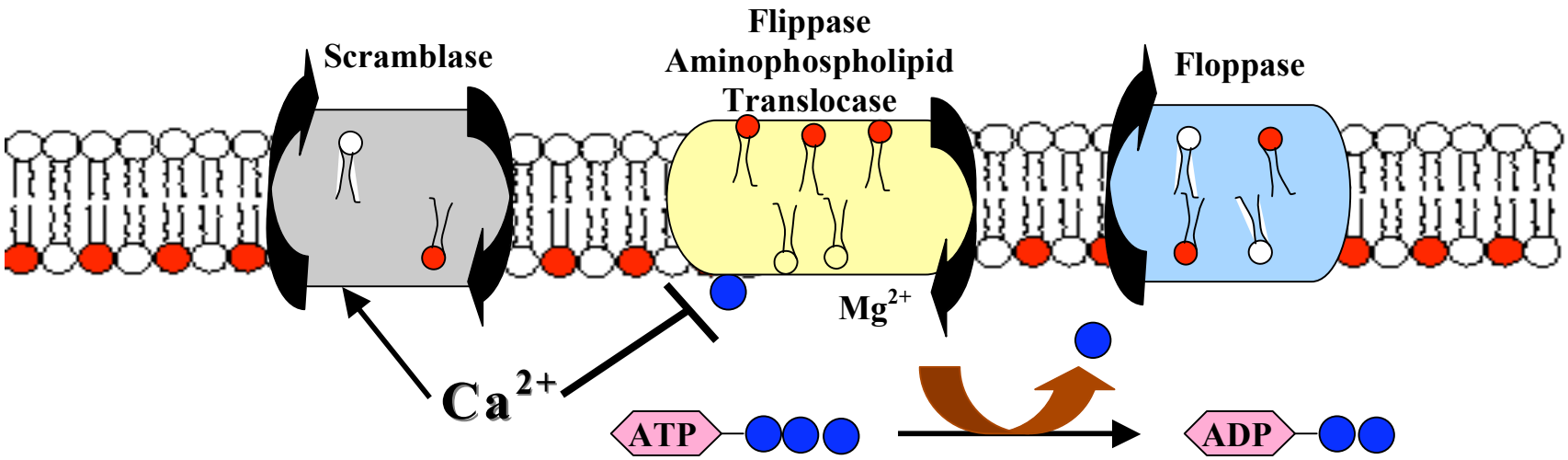

Figure 2: Aminophospholipid Translocase maintains asymmetry by translocating only aminophospholipids, from the outer leaflet of the plasma membrane to the inner. An opposing calcium induced pathway (scramblase) permits all the phospholipids to pass from either leaflet to the other, resulting in the disruption of asymmetry. The APTL protein, is a magnesium dependent P-type ATPase. PS is the optimal substrate. ATPase II, has strikingly similar properties to that of APTL. Mouse ATPase II cDNA was expressed in mouse hippocampal neuron derived HN2 cells to test its effect on APTL activity and other properties of the cells [Zwaal 1997].

P-Type ATPases

As mentioned before, PS is normally confined to the inner leaflet of the plasma membrane by an aminophospholipid translocase (APTL), which specifically transports PS and PE [Zwaal 1997].

The first P-type ATPase activity was discovered in 1957 by Jens C. Skou who was awarded the Nobel Prize in Chemistry in 1997 for his work on the abundant Na^+/K^+-ATPase [Paulusma 2005]. Following this finding, a whole range of different P-type ATPases were identified with varying protein topologies and substrate specificities. Generally, P-type ATPases are important in the generation of cation gradients which make these proteins indispensable in the regulation of cell volume, excitability of nerve cells, muscle contraction, intracellular pH, acid secretion in the stomach, uptake of substrates, and signaling pathways [Paulusma 2005].

Based on phylogenetic analysis, this large family is divided into 5 major subfamilies, each unique in their class of substrates and in subfamily sequence motifs [Axelson 1998, Palmgren 1998]. The type 1 ATPases transport heavy metals such as copper, cadmium, and zinc. The type 2 subfamily transports non-heavy metal cations and includes proteins like the Na^+/K^+, H^+/K^+, and Ca^{2+}-ATPases. The type 3 family includes ATPases only expressed in plants and fungi which are involved in the transport of magnesium and proton ions. Type 4 subfamily members are exclusively expressed in eurkaryotic cells and transport phospholipids. Finally, the recently identified type 5 subfamily – exclusively expressed in eukaryotic cells – only one member of which has been identified so far, is implicated in cellular calcium homeostasis and endoplasmic reticulum function in yeast [Paulusma 2005].

All P-type ATPases share a common topology; usually 10 transmembrane domains, NH_2- and COOH-termini protruding into the cytoplasm, and a large intracellular loop harboring P-type ATPase specific sequences and an ATP binding site [Kühlbrandt 2004]. The core of all P-type ATPases contains a conserved stretch of seven amino acids with the P-type signature sequence 'DKTGT[L,I,V,M][T,I,S].' This motif includes an aspartic acid residue which is reversibly phosphorylated. The formation of this phosphate intermediate is a key feature of these transporters, which are therefore grouped under the name "P-type" ATPases. For several members of the family, it has been shown that an aspartate residue in the DKTG motif accepts γ-phosphate from ATP during the catalytic cycle, forming a covalent acylphosphate intermediate [Kühlbrandt 2004].

The first aminophospholipid translocase activity was described in 1984 in erythrocyte membranes by Seigneuret and Deveaux [Seigneuret 1984]. In 1989, an ATP-dependent translocase activity in chromaffin granules from bovine adrenal glands; spin labeled phospholipid analogs of PS were specifically translocated from the lumenal to the cytoplasmic leaflet of these organelle membranes [Zachowski 1989]. These researchers have hypothesized that an aminophospholipid translocase activity in these Golgi-derived vesicles was necessary to generate fusion-competent, exocytic, vesicles. A few years later, researchers from Auland's lab purified and reconstituted a 110-kDa, Mg^{2+}-dependent, ATPase from human erythrocyte membranes; they demonstrated a 110-kDa-mediated transport activity similar to the activity in chromaffin granules, such as translocation specific for spin labeled PS and to a lesser extent PE [Auland 1994].

In 1996, the gene encoding the chromaffin granular aminophospholipid translocase activity, ATPase II (currently known as ATP8A1), was cloned from a bovine adrenal medulla and thymus cDNA library [Tang 1996]. In the same study, Drs2p, the closest yeast *Saccharomyces cerevisiae* homolog of this protein, was characterized as having a potential plasma membrane aminophospholipid translocase activity; using *Drs2* mutant yeast cells, it was demonstrated that Drs2p was involved in the inward translocation of a fluorescently (NBD)-labeled PS analog NBD-PS ({1-Oleoyl-2-C6-[7-nitro-2-oxa-1,3-diazol-4-yl} amino] caproy1-sn-glycero-3-phosphoserine) across the plasma membrane. Both ATPase II and Drs2p were the first members of a novel subfamily of the P-type ATPase superfamily, the type 4 subfamily [Daleke 2000, Halleck 1998, Halleck 1999, Williamson 2002, Marx 1999, Natarajan 2004, Siegmund 1998].

Mammals express as many as 17 different genes from this subfamily. The type 4 subfamily is divided into 4 classes, 1, 2, 5 and 6 of which members show high sequence similarities, ranging from 23 to 37% sequence identity between proteins of the 4 classes and 43-74% sequence identity between proteins within classes **(Table 1)** [Paulusma 2005]. The pattern of expression of this subfamily in mouse, revealed that these genes are differentially expressed in the respiratory, digestive, urogenital systems, endocrine organs, the eye, teeth, and thymus [Halleck 1999]. One exception is the central nervous system (CNS), where all of the genes are highly expressed, however, the pattern of expression within the CNS differs substantially from gene to gene [Halleck 1999]. These observations suggest that the genes are expressed in a tissue-specific manner. The highly conserved P-type subfamily contains other proteins that transport metal ions such as Mg^{2+}, Cu^{2+}, or Ca^{2+}. Mutations in the FIC1 (Familial Intrahepatic Cholestasis type 1)

gene, which has been described as a member of the P-type subfamily causes two forms of familial inherited cholestasis [Bull 1998]. Also mutations in the copper-transporting ATPase ATP7B lead to a severe multisystem disorder, known as Wilson's disease [Tsivkovskii 2002].

OJECTIVE OF THIS STUDY

Understanding the functional properties of ATPase II that are not known yet and also delineating the structural organization of the gene are set as the main objectives of this study.

This project reveals that ATPase II is indeed an Aminophospholipid translocase or could be involved in the regulation of the translocase activity. In this process we discovered the surprising appearance of calcium current [Chin 2003] and a neuroprotective signaling pathway as a result of overexpression of ATPase II. Analysis of the of ATPase II promoter revealed some cell type specificity of its function. It is important to understand the function and organization of this ATPase II gene in order to test a strategy to trigger phagocytic removal of cancer cells.

Table 1: Tissue Distribution and Chromosomal localization of human type 4 P-type ATPases [Paulusma 2005]

Class	Gene	Protein Name	Chromosomal Localization	Database Accession (*Mouse*)	Tissue distribution
1-∑	ATP8A1	ATPase IA/ATPase II (1164 AA)	4p14-p12	Q9Y2Q0 (*P70704*)	Ubiquitous; high in skeletal muscle, brain; not in liver, lung, testis
1-∑	ATP8A2	ATPase IB/ML-1 (1148 AA)	13q12-13	Q9NTI2 (*P98200*)	*High in testis, low in heart, brain; not in liver, lung, kidney*
1-Φ	ATP8B1	ATPase IC/FIC I (1251 AA)	18q21 – 18q22	O43520 (*NP_001001488*)	Ubiquitous; high in small intestines, pancreas; low in brain
1-Φ	ATP8B2	ATPase ID (1209)	1q21.3	P98198 (*XP_283873*)	Ubiquitous; high in brain, bladder, uterus; not in kidney, skeletal muscle
1-Φ	ATP8B3	ATPase IK (1310 AA)	19p13.3	O60423 (*NP_080370*)	Testis
1-Φ	ATP8B4	ATPase IM (1192 AA)	15q21.2	Q8TF62 (*XP_141343*)	Ubiquitous at moderate levels including, brain, liver, kidney, testis
2	ATP9A	ATPase IIA (1047 AA)	20q13.1 – q13.2	O75110 (*O70228*)	Ubiquitous at moderate levels; not in spleen
2	ATP9B	ATPase IIB/Hussy-20 (1095 AA)	18q23	O43861 (*P98195*)	*Ubiquitous; high in Testis; not in spleen, muscle*
5	ATP10A	ATPase VA (1499 AA)	15q11 – q13	O60312 (*O54827*)	Ubiquitous; high in brain, kidney, lung, pancreas; not in small intestine
5	ATP10B	ATPase VB (1461 AA)	5q34	O94823 (*CAI26159*)	Low in brain and testis

Table 1 (Continued): Tissue Distribution and Chromosomal localization of human type 4 P-type ATPases [Paulusma 2005]

Class	Gene	Protein Name	Chromosomal Localization	Database Accession (*Mouse*)	Tissue distribution
5	ATP10D	ATPase VD (1426 AA)	4p12	Q9P241 (*NP_700438*)	Ubiquitous, moderate in liver, kidney, spleen, ovary; low in brain
6	ATP11A	ATPase IH (1134 AA)	13q34	P98196 (*P98197*)	Ubiquitous; moderate in liver, heart, kidney, muscle, low in brain, spleen
6	ATP11B	ATPase IF (1177 AA)	3q27	Q9Y2G3 (*XP_3588349*)	Ubiquitous (low); moderate in kidney
6	ATP11C	ATPase IG (1132 AA)	Xq27.1	NP_775965	Ubiquitous; high in liver, pancreas, kidney; low in brain, skeletal muscle

Chapter 2

Materials

Reagents:

The GeneRacer™ Kit for full-length, RNA ligase-mediated rapid amplification of 5′ ends (RLM-RACE), the TOPO-TA™ Cloning Kit and Thermozyme™ thermostable DNA polymerase, the THERMOSCRIPT™ RT-System, the Platinum® Taq High Fidelity thermostable DNA polymerase, Agarose and a dNTPs mixture were purchased from Invitrogen Corporation (Carlsbad, CA). Proteinase K (fungal) was purchased from Gibco BRL (currently Invitrogen). Prior to use, proteinase K was dissolved in 10mM Tris-Cl (pH 7.5)-20mM $CaCl_2$-50% glycerol and stored in single use aliquots at -20ºC. The QIAprep Miniprep plasmid DNA isolation kit, QIAquick PCR purification kit, QIAquick gel extraction kit, the Effectene™ Transfection Reagent, RNeasy Mini kit including QIAShredder™ columns and on-column DNase digestion kit were purchased from QIAGEN (Valencia, CA). The pGL3-Basic (no promoter) and pGL3-Promoter (SV40 promoter) firefly luciferase reporter plasmids, pRL-TK vector and the Dual luciferase reporter (DLR) assay kit were purchased from Promega (Madison, WI). All other reagents were obtained from various reputable companies and were of the purity grades deemed appropriate for their respective use.

Animals.

Mice used in these studies were obtained from Taconic and kept in CSI Animal Facility and given food and water *ad libitum*. Mice: for gDNA isolation C57 mouse was used. For RNA isolation we used Swiss Webster wild type mouse.

Methods

Primer Design:

In order to select PCR primers of specific length and temperature of annealing, we used the "RAWPRIMER" program (http://alces.med.umn.edu/rawprimer.html) - this site is no longer available but was used to design the primers used for this project. Primers were analyzed for the presence or absence of stems or hairpin loops using the "Primerdesign" software (http://www.cybergene.se/primer.html). The forward and reverse primers contained specific restriction sites (underlined plus three protecting bases). Addition of restriction sites enables us to perform directional cloning of the PCR products into the vectors of interest (pGL3 Basic – Promega Corporation, Madison, WI; and pcDNA6/Myc-His A – Invitrogen, CA), as illustrated by **Table 2**.

Table 2a- Primers used for Amplification of Full, Distal, Core and Deletion fragments of the Core Promoter

Name	Sequence (5' to 3')	Purpose
-1026 (Forward)	CGG **GGT ACC** AAA GCC TTG CTA CAG GCT CTT TCC G	**Forward Primer for Full/Distal Promoters**
-299 (Reverse)	CTA **GCT AGC** CAA TGC GAT AGA ACC GAC CGT CC	**Reverse Primer for Distal Promoter**
-318 (Forward)	CGG **GGT ACC** CGG TCG GTT CTA TCG CAT TGT AGA GC	**Generation of serial deletions of the ATPase II promoter.**
+193 (Reverse)	CTA **GCT AGC** GGG ACC CTG CAC CTG TCA CG	**Serial deletions were generated using forward primers and +148 reverse primer.**
-270 (Forward)	CGG **GGT ACC** CAG AGC TTT CAG AGC TAA AGA AGC	**Each forward primer contained a *Kpn I* site**
-218 (Forward)	CGG **GGT ACC** ACT TGT ACT GGC CTC AAG GAG G	**And the reverse primers contained an *Nhe I* site at the 5' end.**
-172 (Forward)	CGG **GGT ACC** AAT GCT AGA TCG AAG TCC CCT CC	**The role of the restriction site is to**
-119 (Forward)	CGG **GGT ACC** ACC TGG AGG CTC GGC GGC CCT GTC C	**fascilitate directional cloning into pGL3 basic vector.**
-70 (Forward)	CGG **GGT ACC** AGT GAG CGC GCG CCC CGC AGA CC	
-13 (Forward)	CGG **GGT ACC** AGC CCG CTC CTC TGC CAC TGC	
+33 (Forward)	CGG **GGT ACC** ACG CAG CTC CTT CGC CGC CTT CC	

Table 2b – Primers Used in Amplifying Mouse ATPase II cDNA for Overexpression Studies

Name	Sequence (5' to 3')	Purpose	Source
Fwd-mATPase-HindIII	CCC **AAG CTT** CGA GAC CCA CCT GCA GGG GCT GTC GAG	**mATPase II –pcDNA6A/myc-His construct preparation.**	**NM_009727**
Rvs-mATPase-SalI	TTG AC **GTC GAC** CCA CTC ATC GGG CCT CTG TTT C	**In frame mATPase II – pcDNA6A/myc-His construct preparation.**	**NM_009727**

Table 2c – Primers Used in obtaining 5' RACE products

Name	Sequence (5' to 3')	Purpose	Source
GeneRacer™ 5' Primer	CGA CTG GAG CAC GAG GAC ACT GA		Invitrogen GeneRacer™ Kit
GeneRacer™ 5' Nested Primer	GGA CAC TGA CAT GGA CTG AAG GAG TA		Invitrogen GeneRacer™ Kit
GSP1_NM_009727.exon3	GGAGCAGGGCAATAAAGAGAAAGAACG	Obtaining 1° PCR Product for 5'RACE	NM_009727
GSP_ NM_009727.exon2	AGCGAGGTCTTCTCTGAAACATCATCTG	Obtaining 2° PCR Product for 5'RACE	NM_009727

Table 2d- Primers Used for Sequencing of Promoter Constructs

Name	Sequence (5' to 3')	Purpose	Source
-669F	TGG GAA GTA CGG ACT CAC AC	**Sequencing of**	**Mouse Genome Project March 2005**
-629F	TCC AGT GGC TTC AGG TCT CA	**Full**	**Mouse Genome Project March 2005**
-190R	CCA CCT CGG CCC TCC TTG AG	**Promoter**	**Mouse Genome Project March 2005**
-100R	ACA GGG CCG CCG AGC CTC CA	**Construct in**	**Mouse Genome Project March 2005**
RVprimer3	CTA GCA AAA TAG GCT GTC CCC	**pGL3 – Basic**	**Promega**
GLprimer2	CTT TAT GTT TTT GGC GTC TTC	**Vector**	**Promega**
M13R Universal Primers	GGA AAC AGC TAT GAC CAT G	**Sequencing of**	**Invitrogen**
M13F (-20) Universal Primers	GTA AAA CGA CGG CCA GT	**All Promoters**	**Invitrogen**

2e – Primers used for Sequencing of Mouse ATPase II Constructs

Name	Sequence (5' to 3')	Source
NM_009727.sF207/21	CTA TTC TCA GTT CCG AAG AGC	NM_009727
NM_009727.sr669/20	ACT TTC ACA CTC GAT TCT GC	NM_009727
NM_009727.sr870/21	CAC ATT GGA GAG TTT AAG TGG	NM_009727
NM_009727.sF920/20	GGG AAC ATA AGG CTT GAT GG	NM_009727
NM_009727.sF1400/20	CAA TGA TGG CCG TCT GCC AC	NM_009727
NM_009727.sr2020/20	GCT TGT CCC CAG TAA GGA TC	NM_009727
NM_009727.sr2610/20	CTG TCC AGA AAA GCC GTT GA	NM_009727
NM_009727.sF3343/21	AAC CTG CTT CAC GGC TAT GCT	NM_009727
NM_009727.sr3361/20	CAT AGC CGT GAA GCA GGT TC	NM_009727

Aminophospholipid translocase assay:

APTL assays were conducted according to reported procedures [Hanada 1995, Sleight 1989]. Briefly, the cells were washed twice with HEPES buffered saline (HBS) (20mM HEPES, 137 mM NaCl, 2.7 mM KCl, 0.32 mM Na_2HPO_4, 1.3 mM $CaCl_2$, 0.8 mM $MgSO_4$, 5.5 mM glucose) and then incubated at 37° C in 2 ml of HBS for 5 min. Following this, 1 ml vesicles containing 20 μM NBD-PS ({1-Oleoyl-2-C6-[7-nitro-2-oxa-1,3-diazol-4-yl} amino] caproy1-sn-glycero-3-phosphoserine) (Avanti Polar Lipids, Inc.) and 40 μM PC were added to the overlayer of 2 ml HBS. After gentle mixing, the cells were incubated at 37 °C for 10 min and then the plates were placed on ice. Next 1 ml of an ice-cold solution of 2% bovine serum albumin (BSA) in Krebs Ringer buffer (KRB) (25 mM HEPES, 20 mM glucose, 5 mM KCl, 1.28 mM $CaCl_2$, 1.2 mM $MgCl_2$, 145 mM NaCl, pH 7.4) was added to each plate followed by aspiration. The cells were then incubated on ice for 5 min with an additional 2 ml of ice cold KRB plus 2% BSA. This process of back extraction with BSA solution was repeated two more times to wash off all the NBD-PS that was not flipped to the inner leaflet by APTL. The cells were next washed three times with ice-cold phosphate buffered saline (PBS) (3 ml/ wash) and then harvested in ice-cold PBS. After cell counting, aliquots containing equal number of cells from each sample were added in a total volume of 100 μl to the wells of a 96-well plate for fluorescence reading. Each sample was read in triplicate using a fluorescence plate reader set at excitation and emission wavelengths of 485 nm and 530 nm.

Modified APTL Assay:

Fluorescence tagged 7-nitro-2, 1, 3- benzoxadiazol-4-yl (NBD)-PS vesicles were prepared by dissolving NBD-PS and Phosphatidylcholine (PC) in chloroform: methanol to form 20 µM PS and 40 µM PC (2:1), and used for this light-sensitive experiment. Hepes Buffer Saline (HBS), composed of 20 mM Hepes, 137mM NaCl, 2.7mM KCl, 0.32 mM Na_2HPO_4, 1.3 mM $CaCl_2$, 0.8 mM $MgSO_4$, and 5.5 mM glucose, was used to wash the cells in the 96 well plates. A 2% Bovine Serum Albumin (BSA) solution in Krebs Ringer Buffer (KRB), composed of 124 mM NaCl, 3.1 mM KCl, 1.3 mM KH_2PO_4, 1.3 mM $MgSO_4$, 3.1 mM $CaCl_2$, 25.9 mM $NaHCO_3$, and 10.0 mM glucose, was prepared by adding 1g of BSA to 50 mL of KRB. This solution was necessary in order to bind to lipid vesicles that had congregated on the outer membrane of the cell and had not been internalized. Phosphate Buffer Saline (PBS), composed of 137 mM NaCl, 2.7 mM KCl, 4.3 mM Na_2HPO_4, and 1.47 mM KH_2PO_4, was used to wash cells and also to obtain background readings of fluorescence.

The APTL assay was later standardized for 96 well plates. Cells were plated and grown to approximately 80% confluence in a black-walled, 96 well, clear-bottomed assay plate. The cells were washed twice with 20 µl of HBS, aspirated, and then coated with 10 µl of HBS. After this they were placed in a water bath at 37°C for 5 minutes. Following the 5 minute incubation, the NBD tagged PS (2:1) vesicles were added at 4 µl per well. The lipid vesicles were incubated for a variety of time periods, most commonly 0',1',3',5',7',10',12', and 15'. After the incubation of the lipid vesicles, the plate was quickly transferred to an ice water bath, where 4 µl of the 2% BSA+KRB solution was added to each well and aspirated immediately. The cells were then washed 3 times with

2% BSA in KRB with 10 minute incubations in between each wash. Following the BSA back extraction of excess lipid vesicles, the cells were washed with 10µl of PBS 3 times. On the third PBS wash, 100µl of PBS was added to each well. The fluorescence in each well was then monitored using a fluorescence plate reader (excitation 485, emission 528).

Protein Normalization:

When APTL assays were run with several different cell lines on one assay plate, each cell line had a tendency to multiply at a different rate. Because of this, the amount of fluorescence could not be compared among different cell samples without normalizing the assay to the amount of protein. The cells were lysed using RIPA buffer (PBS containing 1% Nonidet P-40, 0.5% sodium deoxycholate, and 0.1% SDS) which was supplemented with the following agents: 25x Protease and Phosphatase Inhibitor cocktail, 200µM Na_2VO_4, 500µM NaF, 100µM $Na_4P_2O_7$, 500µM EDTA, and 250µM PMSF (1000x). After lysing, they were either stored in a -20°C freezer, or prepared for protein estimation. Each sample of 10µl was prepared in duplicates with 65µl of distilled H_2O. 25µl of Reagent A, which is an alkaline copper tartrate solution, were added to each sample, as well as 200µl of Reagent B, which is a Folin reagent. After 15 minutes of incubations, the samples were vortexed and then read in a spectrophotometer at 750 nm.

Optimization of dithionite treatment:

Dithionite reduces 7-nitro-2, 1, 3- benzoxadiazol-4-yl labeled lipids to 7-amino-2, 1, 3-benzoxadiazol-4-yl-labeled lipids. This removes the NBD label from PS, thereby quenching fluorescence. This procedure was run in addition to the BSA back extraction method, in which the lipid vesicles bound to the BSA. As a result of back extraction, the vesicles on the outer leaflet of the membrane were washed away; however, this fluorescence removal on the outer leaflet was not sufficient. Dithionite treatment was performed in order to ensure the quenching of fluorescence on the outer leaflet of the cell membrane, leaving fluorescence to be emitted only from the inner layer. This provides more accurate results in measuring the PS internalization in a cell.

NIH3T3, B16F10, and HN2 Cells were plated in black-walled, clear bottom 96 well plates for a dithionite based assay. The cells were washed twice with 20µl of HEPES Buffer Saline (HBS) and then incubated for 5 minutes in 8µl of HBS. Following the 5 minute incubation, 4µl of PS tagged with fluorescent NBD vesicles (NBD-PS) were added to each well. The cells were then incubated for 10 minutes in a 37 °C water bath, during which the NBD-PS vesicles integrated with the plasma membranes of the cells. Immediately following the incubation, the plates were moved from the water bath to an ice water bath in which they were treated with 4µl of a KRB + 2%BSA solution. After aspiration, vesicles were again back extracted by incubating with 8µl KRB +2%BSA for 3 minutes on the ice water bath followed by aspiration. 1.0 mM Sodium Dithionite in 1.0 mM Tris was added to each well in a time course using 10, 5, 3, 1, and 0 minute time points. The wells were then aspirated and washed 3 times with 13µl of Phosphate Buffer Saline (PBS) per well and scanned using a fluorescence plate reader.

SDS-PAGE and Immunoblot analysis:

The cell or tissue pellets were homogenized on ice in RIPA buffer (PBS containing 1% NP40, 0.5% sodium deoxycholate, 0.1% SDS, 0.5 mM Na_3VO_4 plus freshly added protease inhibitor cocktail; Boeringer) and then assayed for protein concentration. For the analysis of ATPase II, aliquots containing 50 µg and 100 µg protein from each were placed in the treatment buffer and then heated in a boiling water bath for 5 min.sample were followed by resolution on 7-16% gradient SDS-polyacrylamide gel. The resolved proteins were transferred to nitrocellulose membrane and then probed with a rabbit polyclonal antibody directed toward the N-terminal region of ATPase II (antibody B; reference number 2616). The nitrocellulose membrane is blocked overnight (at 4 °C) with 10% milk in 0.1% Tween-TBS, then treated with 1: 10,000 dilution of the ATPase II antibody in fresh blocking solution, washed three times with Tween-TBS, treated with peroxidase-linked antimouse IgG (1: 20,000), washed, and then the protein bands were detected using the Dura kit (Pierce). Following this, the blots were stripped by incubating at room temperature for 1 h in a stripping buffer (0.25 M glycine, pH 2.0), blocked again and then probed with 1: 10,000 dilution of a monoclonal ß-Actin antibody (Sigma). The secondary antibody concentration maintained in this case was 1: 50,000.

Caspase-3 Assay:

Caspase assays were performed using monolayers of HN2 and the ATPase II overexpressing clones A12 and A22 cells at 80% confluence. Cell lysates were prepared from hydrogen peroxide-treated or normoxic and anoxic cell pellets obtained after two washes with ice-cold PBS. Cells were next lysed in 0.5 mL Yama buffer (10 mM HEPES

pH 7.5, 142 nM KCl, 1 mM EGTA, 1 mM DTT, 0.2 % NP-40, 0.1 mM PMSF) [Deveraux 1997]. Each sample was homogenized with a Potter Elvehjem homogenizer and then ultracentrifuged at 100,000 x g for 5 minutes. The supernatant obtained was assayed for protein concentration, which was adjusted to 10 µg/µl and then an aliquot containing 300 µg protein was added to each well of a 96-well plate. This was followed by the addition of 1.5 µl of 10 mM stock AcDEVD-AMC in oxygen-free water (final concentration, 100 µM). the released fluorescence (due to the fluorescent group, AMC, which is cleaved by the caspases) was monitored after 30 minutes incubation using a fluorescent plate reader set at excitation wavelength 360 nm and emission wavelength 460 nm. Each caspase assay was performed with triplicate samples.

Analysis of the 5'-untranslated sequences by RLM-RACE:

Total RNA samples (5 μg each) obtained from mouse brain, heart, lung, kidney, liver and spleen (SwissWebster Mouse), were processed for RLM-RACE using the GeneRacer™ (Invitrogen, CA) kit as detailed in the manufacturer's protocol. The RNA samples were dephosphorylated in the presence of 10 U of calf intestinal phosphatase (CIP) at 50°C for 1 hour. Following purification of the RNA sample by ethanol precipitation, the mRNA cap structure was removed by treating the dephosphorylated RNA with 0.5 U of tobacco acid pyrophosphatase (TAP). The decapped mRNA was purified and then ligated in the presence of T4 ligase (5U) to an adapter RNA oligonucleotide sequence that was specific for both the GeneRacer 5' Primer and the GeneRacer 5' Nested primer. An aliquot of the purified ligation product, containing approximately 2 μg of RACE-ready RNA, was reverse transcribed in the presence of an oligo dT primer using 200 U of SuperScript™ III RT (Invitrogen, CA). The product was subsequently treated with 2 U of RNase H at 37 °C for 20 minutes and then the cDNA product was used immediately for PCR amplification. PCR amplification was performed first with the GeneRacer 5' Primer and and *ATPase II*-specific primer NM_009727.exon3 **(Table 2).** The conditions of PCR were 94 °C/2 minutes followed by 5 cycles of 94 °C/30 seconds, 62 °C/30 seconds, 68 °C/2 minutes, followed by another 5 cycles of 94 °C/30 seconds, 60 °C/30 seconds, 68 °C/2 minutes, followed by 25 cycles of 94 °C/30 seconds, 58 °C/30 seconds, 68 °C/2 minutes, finally followed by an extension at 72 °C/10 minutes. An aliquot containing 4% of the primary PCR product was then reamplified using the GeneRacer 5' Nested Primer and a second *ATPase II*-specific primer NM_009727.exon2 **(Table 2)**. The conditions of

PCR were 94 °C/2 minutes, followed by 25 cycles of 94 °C/30 seconds, 63°C/ 30 seconds, 68 °C/1 minute, and a final extension at 68 °C/10 minutes.

Organization of the *ATPase II* Gene:

In order to elucidate the chromosomal organization of the *ATPase II* gene, we compared sequences of *ATPase II* cDNAs NM_009727, AK220560, AK045367 and AK076388 to Human Genome Sequence using the Human Genome Browser (http://genome.ucsc.edu/ [Kent 2002]) The data presented in this report has been obtained using assembly as of March 2005, which is the most recent version. Whenever necessary, sequences were aligned manually using standard word processing software and visually inspected.

Searching for the potential promoter region and transcription factor binding sites in the *ATPase II* Gene:

The search for the potential promoter region in the *ATPase II* gene was performed via the internet using GenomatixSuite collection software (Genomatix Software GmbH, Munich, Germany) available at http://www.genomatix.de. The PromoterInspector [Scherf 2000] mammalian promoter prediction software was used to analyze the 5' end of the *ATPase II* gene for the presence of the promoter and the MatInspector [Quandt 1995] to identify the potential transcription factor binding sites. We isolated a 1.4 kb upstream sequence of the ATPase II gene using the first exon as a probe for sequence comparison against the mouse genome. About 12 kb of this sequence was analyzed using the online software PROMOTERINSPECTOR in the package MATINSPECTOR (http://www.genomatix.de) and also the sequence was compared with other promoter sequences, which identified ≈ 1.4 kb 5'-flanking sequence as the promoter for this gene.

PCR Amplification of Promoter Fragments:

The promoter fragments were initially PCR amplified from 100 ng of genomic DNA per sequence amplified. A 50 µl reaction contained the following: 5 µl of 10 X HiFi buffer, 2 mM $MgSO_4$, 0.2 mM dNTP mix, 2 µM Forward primer (Full- FF, Distal- DF, or Core- CF), 2 µM Reverse Primer (Full- FR, Distal- DR, or Core- CR), 1.5 U of Platinum HiFi Taq polymerase , 2.5 µl PCR_x enhancer (this was used in amplifying the full and core promoters due to the GC rich region of the core promoter). PCR conditions were 96 °C for 2 minutes, 94 °C for 2 minutes, 5 cycles of 96 °C for 45 seconds, 64 °C for 30 seconds, 68 °C for 1 minute, then 28 cycles of 95 °C for 45 seconds, 61 °C for 30 seconds, 68 °C for 1 mintue; finally 72 °C for 10 minutes.

DNA Sequencing:

The sequencing of the clones were done commercially by ACGT, Inc (Wheeler, IL). The promoter fragments, 5'RACE and the mouse ATPase II-pcDNA6A/Myc-His construct were sequenced in both directions using universal forward and reverse primers. Each clone was sequenced on both strands, and for the larger constructs we performed more sequencing using additional internal primers**.**

Transient transfection studies of the APTL promoter:

Cells grown to 30% confluence in a 24-well plate were washed with serum-free DMEM and then treated with the following transfection mixture (using a Qiagen transfection kit): Plasmid DNA (0.2 µg) + EC buffer (60 µl) + Enhancer (1.6 µl)➔ Mixed and incubated for 5' at room temperature. Effectene (5 µl) added, mixed and incubated for 10' at room temperature. Finally, DMEM (10% FBS, 1% PS) (350 µl) added, mixed and the reagent

mix added to one well of cells overlayered with 350 µl of DMEM (10% FBS, 1% PS). After 3 h at 37 °C, the medium was replaced with 1 ml regular growth medium (DMEM plus 10% FBS, 1% PS) and then the cells were allowed to grow for 48 h. Next, cells were washed with PBS and lysed in 200 µl 1x Passive lysis buffer (PLB) included in the Dual luciferase reporter (DLR) assay kit (Promega) and 20 µl of each lysate was added to 100 µl of luciferase assay reagent (LAR II). After mixing, initial luminescence was measured within 30 sec using a luminometer. After the first reading, the sample tube was removed from the luminometer and 100µl of 'Stop & Glo' Buffer, which was also included in the kit, was added to the mixture of Luciferase Assay Reagent (LAR) II and lysate.

Transient transfection of antisense APTL cDNA into HN2 cells and detection of externalized PS:

Mouse APTL cDNA was obtained from mouse brain mRNA by RT-PCR. During the PCR amplification, appropriate primers containing the 5'-restriction sites XhoI and ClaI were used and the product obtained was cloned into the TOPO-TA cloning vector pCR4. The contruct obtained was tested by restriction digestion and then digested with XhoI and SalI and released insert containing the APTL cDNA was cloned into SalI and ClaI sites on the vectors pCMV6b (for sense) and pCMV6c (for antisense), which differed only in the opposite orientation of their multiple cloning region. For transfection, HN2 cells grown to 30% confluence in a 24–well plate were washed with serum-free DMEM and then ovelayered with 350 µl of complete growth medium (DMEM+10% FBS+penicillin-streptomycin). Meanwhile, 1.5 µg of each construct (the sense, or the antisense in Fig. 8) was mixed with 0.5 µg of pEGFP (Clonetech, CA), 10 µl of the Superfect reagent, and 60

µl of serum and antibiotic-free DMEM. The GFP control included only 0.5 µg pEGFP. The mixture was vortexed for 10 sec and then incubated at room temperature for 10 min, following which 350 µl of complete growth medium was added to it. After pipet mixing, this DNA:Superfect complex was added to each well of the 24-well plate. The plate was gently swirled and then incubated at 37 °C for 3 h. Next the medium was replaced with fresh complete growth medium and the cells were allowed to grow for 48 h. At this point, the cells from each well were harvested by gentle trituration with PBS, pelleted at 1000 rpm, washed once with PBS and then resuspended in 100 µl of 1X Annexin-Binding Buffer from an Annexin V-Alexa Fluor 350 staining kit (Molecular Probes, OR). Component A (Biotin-X annexin V) (5 µl) was added from the kit to this cell suspension, followed by gentle mixing and incubation at room temperature for 15 min. Next, the cells were pelleted, washed once with Annexin-Binding Buffer, and then resuspended in 10 µl of Annexin-Binding Buffer. An Alexa Fluor 350-streptavidin solution (1 µl of a 1 mg/ml stock) was added to the cell suspension, followed by by gentle mixing and incubation at room temperature for 30 min. The cells were then washed, resuspended in the Annexin-Binding Buffer (100 µl), and 20 µl of this suspension was pipet-mixed with 20 µl of the mounting medium, and the resulting cell suspension mounted on coverslips for fluorescence microscopy. Pictures were taken using a SPOT Model 1.1.0 digital camera (Diagnostic Instruments, Inc.) and the following photo filters: 510-530 nm (emission) to detect GFP expression (green), and 420-440 nm (emission) to detect annexin V staining (blue) of externalized PS.

Transient Transfection of antisense mouse ATPase II.

The main reagent used in this transfection was ExGen 500, a sterile solution of linear polyethylenimine (PEI) molecules in water at a concentration of 5.47mM in terms of nitrogen residues. PEI has a high cationic-charge density potential, which makes it an excellent DNA condensing and gene-delivering agent. The materials used in this transfection were PEI 800 and PEI 50 stock, 100 mM (with respect to Nitrogen), 5% Glucose, 150 mM NaCl, and stock 100 mM PEI 800 and PEI 50 (PEI 800 and PEI 50 should be diluted 10 fold to 10 mM in sterile H_2O). This generally makes 100 µl to 1000 µl of solution. When transfecting with Exgen500, 1µg of plasmid DNA (pDNA) per well was used, while with PEI 800 or PEI 50, 2 µg of pDNA was used per well. The amount of DNA is kept constant, and the amount of PEI is variable. Any 1 µg of pDNA is 3 nmols of phosphate regardless of the size of DNA molecule. In PEI 800, 1 µl of 10 mM solution (Stock diluted 10x) contains 10 nmols of Amine Nitrogen (protonated Nitrogen). For PEI 800 and PEI 50, the ratio was presented as 6:9:13:18, and 2 µg of pDNA (1 µg of Construct + 1 ug of pEGFP-C1) was used. A tube of 1µg of pDNA in 50 µl of total volume of 5% glucose was pipette mixed and set aside. In a second tube, the appropriate amount of EXGEN 500 according to the optimal ratio should be added with the final volume being 50 µl with 5% glucose. The tubes were then incubated at room temperature for 10 minutes. These mixtures are then combined in such a way that EXGEN 500 solution is added to the DNA solution. They were then vortexed immediately. With PEI 800 or PEI 50, there was a 20 minute incubation following this vortexing, where as with EXGEN, there is a 10 minute incubation. In this experiment, procedures were performed at room temperature.

Description of Cells Used Throughout this Thesis:

B16F10 are mouse melanomal cells and were obtained from Dr. Rottenberg (Queens College (Flushing, NY). The mouse hippocampal neuron-derived hybrid neuroblastoma cell line HN2 cells were obtained from the CSI cell depository. N18 (Mouse neuroblastoma cells) were obtained from Dr. Effrain Azmitia, New York University (NY, NY). The SN48.1p cell line was from Dr. Bruce Wainer's lab at the University of Chicago (Chicago, IL). All these cells were cultured in DMEM (Dulbecco's Modified Eagles Medium) containing 10% FBS (Fetal Bovine Serum) and 1% PS (Penicillin-Streptomycin). NIH3T3 cells (generous gift from Dr. Yuan Hwang's lab at NY State Institute For Basic Research (Staten Island, NY) were cultured with DMEM media containing 10% Calf Serum and 1% PS. All cells used in these studies were grown in the incubator set at 37 °C in 5% CO_2.

Chapter 3:

Results

Stable overexpression of ATPase II in hippocampal neuron-derived cells showed a dramatic increase in APTL activity.

Our previous studies have revealed that during the late stages of apoptosis PS is externalized as a result of APTL inhibition [Adayev 1998]. These studies were conducted in hippocampal neuron-derived HN2-5 cells, which were obtained by stable expression of a G protein-coupled receptor in the parent HN2 cells. As a result of the previous studies on apoptosis and PS externalization, we went on to study the effect of overexpressing ATPase II in the parent HN2 cells. This effect was studied by creating a contruct of the mouse ATPase II cDNA. The mammalian expression vector that was used to overexpress ATPase II cDNA was the pCMV6c vector. Mouse ATPase II cDNA was ligated into this vector and the recombinant construct was then transfected into HN2 cells. Two successful clones were created, dubbed HN2A12 and HN2A22. ATPase II overexpression was confirmed by Western blotting (Figure 3). Then APTL activity was measured in these clones. Both clones showing increased ATPase II expression also showed a dramatic increase in APTL activity, as illustrated by Figures 4.

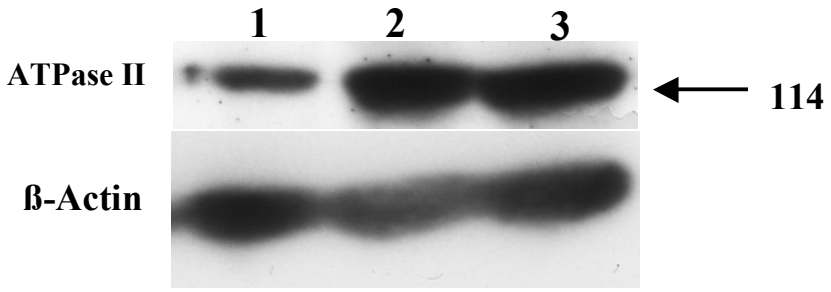

Figure 3: Westernblot analysis using an N-terminal-directed antibody {Also known as Ab B (1:10,000)} showed a dramatic increase in ATPase II expression at 114 kDa in HN2A12 (Lane 2) and HN2A22 (Lane 3) as compared to that in the untransfected HN2 (Lane 1) cells. Each lane received 100 µg of whole cell lysate. ATPase II antibody (Ab B) was obtained from Xiao-Song Xie, Ph.D., UT South Western Medical Center, TX.

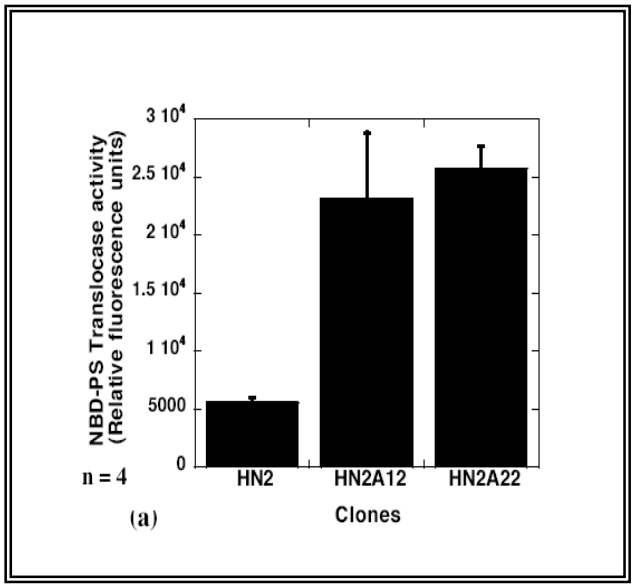

Figure 4: Aminophospholipid translocase assays showed a five-fold increase in activity in the stable transfection HN2-A12 and HN2-A22.

APTL Activity in the ATPase II Overexpressing Cells Was Insensitive to Anoxia/Reoxygenation

To further analyze the role of ATPase II in apoptosis, we conducted APTL assays on another HN2-derived cell-line, HN2-5, and one of the clones overexpressing ATPase II (HN2A12). These cells were subjected to anoxia/reoxygenation, as illustrated by Figure 5.

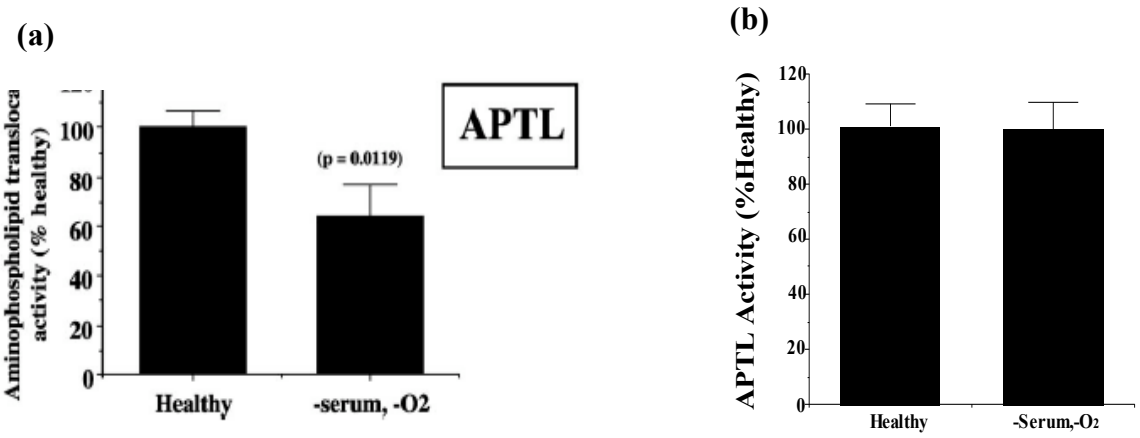

Figure 5: APTL activity in the ATPase II overexpressing cells was insensitive to anoxia/reoxygenation. Differentiated HN2-5 and HN2-A12 were subjected to anoxia/reoxygenation. APTL assay showed that the activity in the stable transfectant HN2-A12 were insensitive to anoxia/reoxygenation and serum deprivation, as opposed to the HN2-5 cells which were subjected to anoxia/reoxygenation and serum deprivation. (a) The sister cell-line (HN2-5) expressing endogenous ATPase II shows inhibition of APTL activity, when subjected to anoxia reoxygenation. (b) There was no change in APTL activity in the ATPase II overexpressing clone (HN2A12) when subjected to the same stress condition as HN2-5.

Stress-mediated activation of Caspase-3 activity is blocked in the ATPase II overexpressing HN2A12 cells.

Our earlier studies have shown that anoxia-reoxygenation of two neural cell lines, including the HN2-derived HN2-5 cells, caused a significant increase in caspase-3 activity and a suppression of APTL activity [Das 2003]. Such induction of caspase-3 was also observed in the HN2 cells after both anoxia—reoxygenation and oxidative stress, triggered by H_2O_2 treatment (Figure 5). In addition, H_2O_2 treatment also caused a significant decrease in APTL activity in the HN2 cells. Remarkably, the H_2O_2 mediated suppression of APTL activity was not observed in the ATPase II-overexpressing HN2A12 cells. Furthermore, caspase-3 activity was not increased above control (Figure 5a) in the HN2A12 cells following both anoxia-reoxygenation as well as H_2O_2 treatment (Figure 6). This strongly suggests that ATPase II blocks apoptosis in the HN2 cells

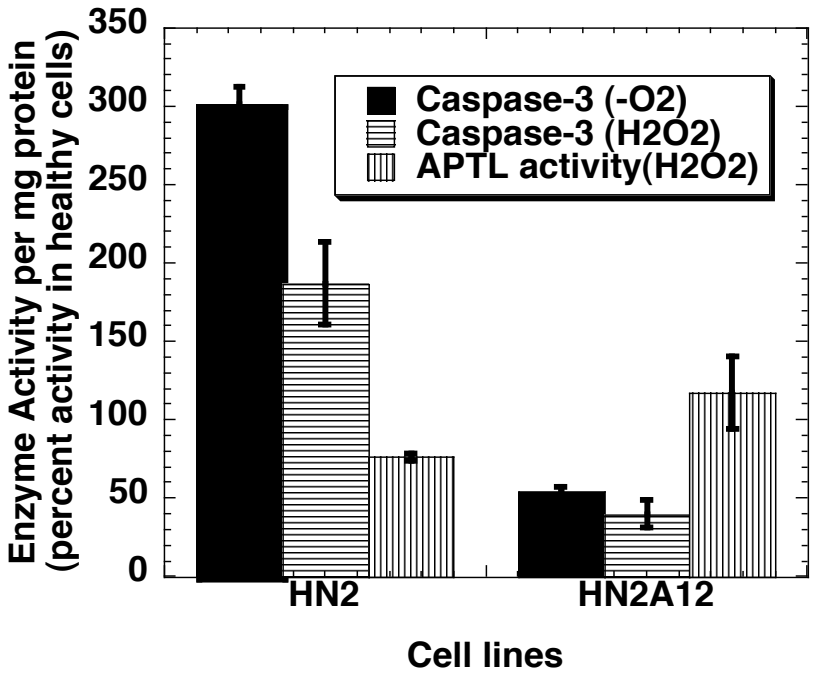

Figure 6: Suppression of caspase-3 activity in ATPase II overexpressing HN2A12 cells. The HN2 and the HN2A12 cells were subjected to 6 hours of anoxia and 16 hours reoxygenation serum-free DMEM. Since •OH radical generated through Fenton reaction during reoxygenation is believed to cause the injury, the cells were also treated with 200 μM H_2O_2 (which generates •OH) for 16 hours. Following this, the cells were either assayed for APTL activity or Caspase-3.

Overexpression of ATPase II shows signal transduction activity by causing persistent activation of Erk 1/2, induction of Fos B and inhibition of caspase-3 activity.

A novel signaling function of mouse ATPase II was discovered in the cells that overexpressATpase II (A12 & A22 cells). Induced expression of the α_{1B} subunit of the N-type Calcium channels and also the induction of voltage-gated calcium currents in both of the ATPase II overexpressing clones HN2A12 and HN2A22 suggested that ATPase II could be at the apex of a signaling cascade that could influence gene expression. This could occur through the MAP (mitogen activated protein) Kinase pathway, consisting of the isozymes Erk 1 and Erk 2 (Erk 1/2), which upon activation cause phosphorylation of transcription factors (e.g. Fos B) that bind to promoters of specific genes to regulate transcription [Bratton 1997]. Remarkably, the ATPase II overexpressing clones HN2A12 and HN2A22 cells showed a three-fold increase in the levels of active Erk 1/2 (Figure 7 Panel) B. Furthermore, an even greater (amplification) increase in Fos B levels in the HN2A12 and HN2A22 cells was observed (Figure 7 Panel C), which is likely a sequel to the activation of Erk 1/2.

Figure 7: Activated forms Erk 1/2 and induced expression of Fos B in the ATPase II overexpressing clones HN2A12 and HN2A22. The blot used to probe for ATPase II was reprobed with antibodies to pErk 1/2 (Cell Signaling, CA) (Panel B), c-Fos (which cross-reacts also with Fos B, Fra-1, and Fra-2). The immunoreactive band (Panel C) had a molecular weight of 35 kDa, which corresponded to Fos B (c-Fos, Fra-1, and Fra-2 have the molecular weights of 55-, 43-, and 42 kDa, respectively). Normalization of band intensities was carried out with respect to the ß-Actin bands (Panel D).

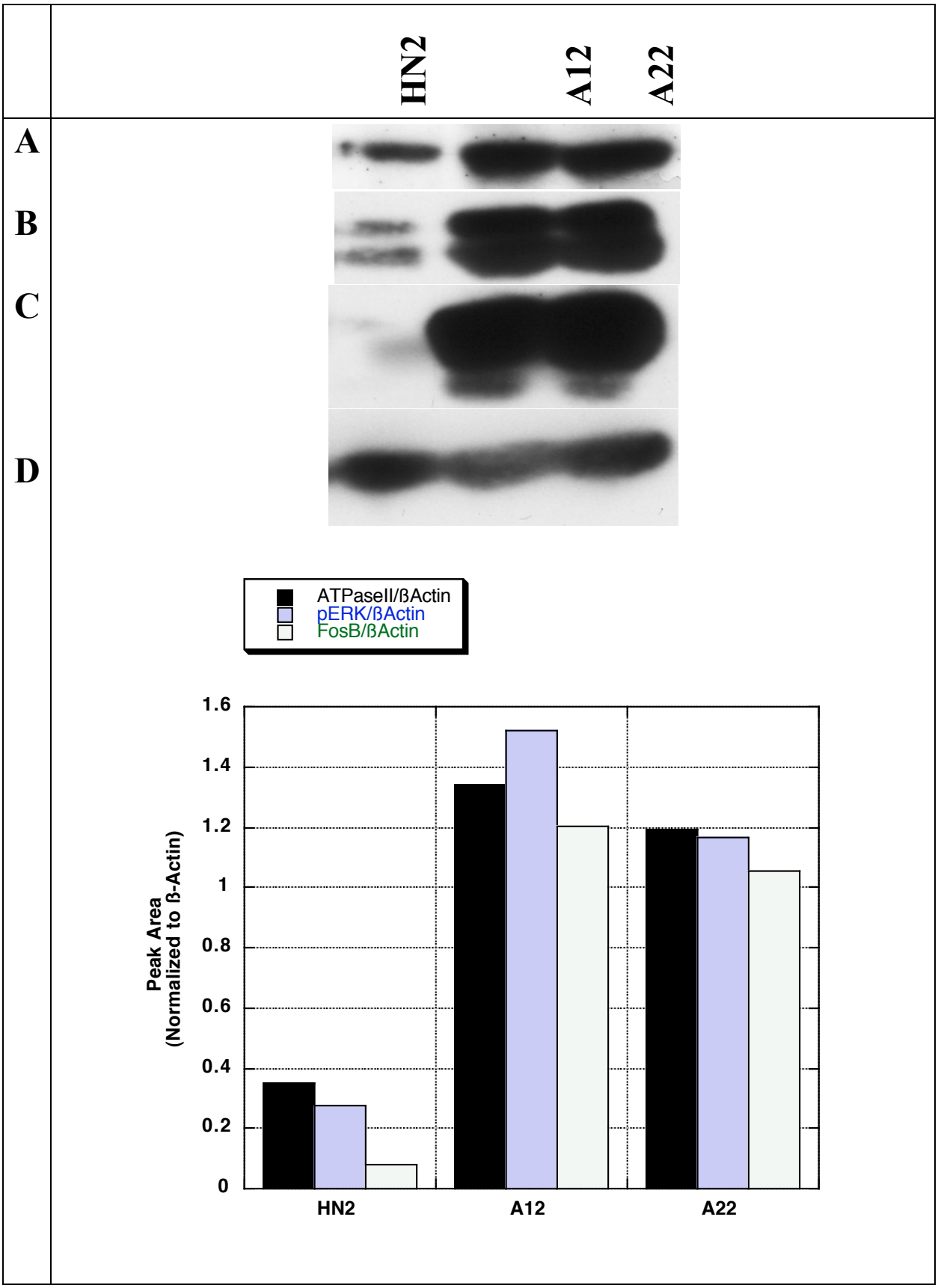
HN2
A12
A22
A
B
C
D
ATPaseII/ßActin
pERK/ßActin
FosB/ßActin
Peak Area
(Normalized to ß-Actin)
1.6
1.4
1.2
1
0.8
0.6
0.4
0.2
0
HN2
A12
A22

Aminophospholipid Translocase (APTL) activity is increased in B16F10 cells transiently expressing mouse ATPase II.

A dithionite based assay using 10' of incubation with NBD-PS, and 5' of incubation with dithionite solution, was run using over-expressing mATPaseII clones of B16F10 cells B16F10 mATPase II clones showed a significant increase in APTL activity. In each cell line, there was at least a 1.5 fold increase in APTL activity.

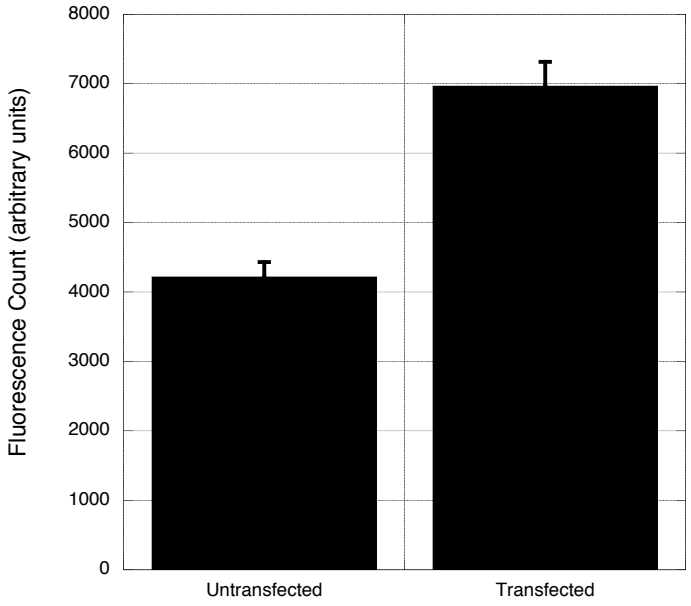

Figure 8: A mATPase II over-expressing clone shows an increase in APTL activity. B16F10 mATPase II clones were run in a dithionite based APTL assay. Untransfected cells were used in comparison to over-expressing transfected mATPaseII constructs.

Transient transfection of full-length, antisense ATPase II cDNA causes externalization of PhosphatidylSerine (PS).

The protein annexin V selectively binds to PS, and this property is generally used in monitoring PS externalization. Annexin V covalently linked to a fluorophore thus binds to PS-externalized cells, which are then easily identified by fluorescence microscopy [Adayev 1998]. If indeed ATPase II is central to the inner membrane localization of PS then inhibition of the function ATPase II or a decrease in expression of this enzyme would cause externalization of PS. Other research teams have tested this hypothesis earlier using inhibitors of APTL [Gleiss 2002]. In these studies, the function of APTL was inhibited either by increasing intracellular Ca^{2+} concentration or by depleting intracellular ATP, both of which cause inhibition of APTL activity. However, changes in the concentration of such moieties that regulate a very large number of biochemical pathways in a cell could result in many other changes in a cell. Alternatively, antisense sequences could be used specifically to suppress expression of a target gene [Benimetskaya 2001, Myers 2000]. Such sequences either bind directly to the target RNA sequences or produce transcripts that form double-stranded RNA with the target RNA. Such double-stranded RNA sequences are readily digested by RNAaseH. Although, generally, short-length, antisense, phosphorothioate oligonucleotides (S-oligos) are either added to or transfected into cells to suppress the expression of a gene, some studies have also shown that expression of the antisense version of a full-length gene can selectively silence a gene [Glondu 2002, Kadonaga 1987, Laplante 2000]. However, such long-chain antisense RNA sequences can produce an unwanted interferon response in a multicellular organism [Kunsch 1992]. Since we have a clonal, neurotumor cell line, in our preliminary study, we conducted a primary test of feasibility of the idea

of expressing an ATPase II-silencing sequence to cause PS externalization. As shown in Figure 9, transient transfection of a full-length antisense APTL cDNA sequence in the hippocampal neuron x N18 neuroblastoma cell line, HN2, causes externalization of PS, as monitored by Annexin V-Alexa Fluor 350 staining (blue) (Fig. 9 i-viii). The cotransfected pEGFP construct results in the expression of the green fluorescent protein (GFP) (Fig. 9 ii, iv, vi, viii, x, and xi) in the transfected cells. Transfection of either pEGFP alone or the APTL sense strand along with pEGFP did not produce any significant Annexin V-Alexa Fluor 350 staining in the healthy and GFP-expressing cells (Fig. 9 ix). Only a few apoptotic cells showed PS externalization (marked by Annexin V-Alexa Fluor 350 staining-blue) among the sense APTL-transfected cells (e.g. Fig. 9 ix and x). A higher magnification view of two healthy transfected with pEGFP plus sense APTL is shown in Figure 9xi, but these cells showed no Annexin V-Alexa Fluor 350 staining (the image was too dim for capture by the digital camera). Similar transfection was carried out with pEGFP alone to obtain essentially the same results as shown for the sense APTL-transfected cells (data not shown here).

In this experiment, we analyzed four fields of view for each sample, i.e. twelve fields in a triplicate set. Results shown in Figure 9 were dramatic and they strongly supported the feasibility of the idea that abrogation of ATPase II expression could cause PS externalization in neurotumor cells.

Figure 9: Transfection of antisense ATPase II cDNA causes PS externalization in HN2 cells. ATPase II cDNA was amplified by RT-PCR from mouse mRNA and then ligated in sense and antisense orientations into the vector pCMV6b and pCMV6c (only the multiple cloning region is inverted in these two vectors). The sense and antisense ATPase II vectors were each cotransfected with pEGFP into HN2 cells in triplicate wells of a 24-well plate (see methods). After 48 hours, the cells were harvested and then stained using an annexin V-Alexafluor350 kit (Molecular Probes, OR). Stained cells were mixed with mounting medium (90% glycerol and 0.1% paraphenylene diamine) and then mounted on cover slips for fluorescence microscopy. Pictures were taken using a Nikon inverted microscope fitted with a digital camera, connected to a computer. **Antisense: (i), (ii), (vii),** and **(viii)** show low-magnification views (20,000x) of clusters of transfected cells displaying GFP fluorescence (green) (510-nm filter) and also Annexin V staining (blue) (420-nm filter). **(iii)** and **(iv)** show higher magnification (40,000x) of a healthy cell showing both GFP fluorescence **(iv)** as well as annexin V staining **(iii).** At the highest magnification (60,000x), **(v)** and **(vi)** show GFP fluorescence **(vi)** in the cytoplasm and surface annexin V staining **(v)** in a healthy but transfected cell. Similar analysis of the **sense APTL**-transfected cells show annexin V staining of only one apoptotic cell **(ix)** in the midst of a cluster of GFP-expressing, transfected cells **(x)**. The sense APTL transfected, healthy cells shown in **(xi)** displayed no annexin v fluorescence and thus this field of view was too dim for capture through the 420-nm emission filter (also, see Methods).

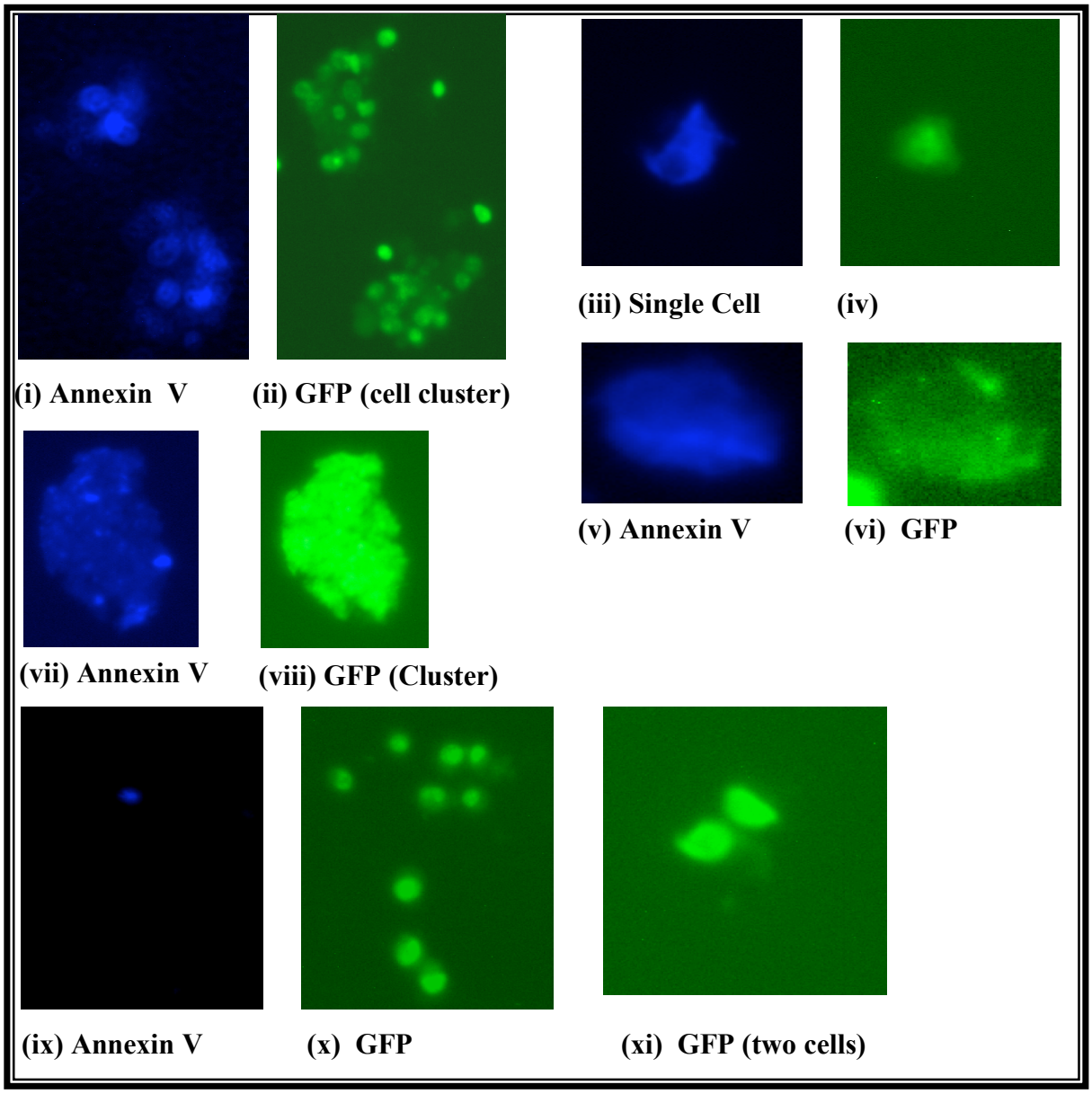
(i) Annexin V
(ii) GFP (cell cluster)
(iii) Single Cell
(iv)
(v) Annexin V
(vi) GFP
(vii) Annexin V
(viii) GFP (Cluster)
(ix) Annexin V
(x) GFP
(xi) GFP (two cells)

Transient transfection of Antisense ATPase II show suppression in APTL activity. B16F10 cells were transfected with the mATPase II Antisense vector using the transfection reagent PEI. The antisense vector is converse to the over-expressing mATPase II vector; therefore, it under-expressed ATPase II in B16F10 cells. There was a concomitant inhibition of APTL activity. These two experiments strongly indicate that ATPase II is indeed an APTL.

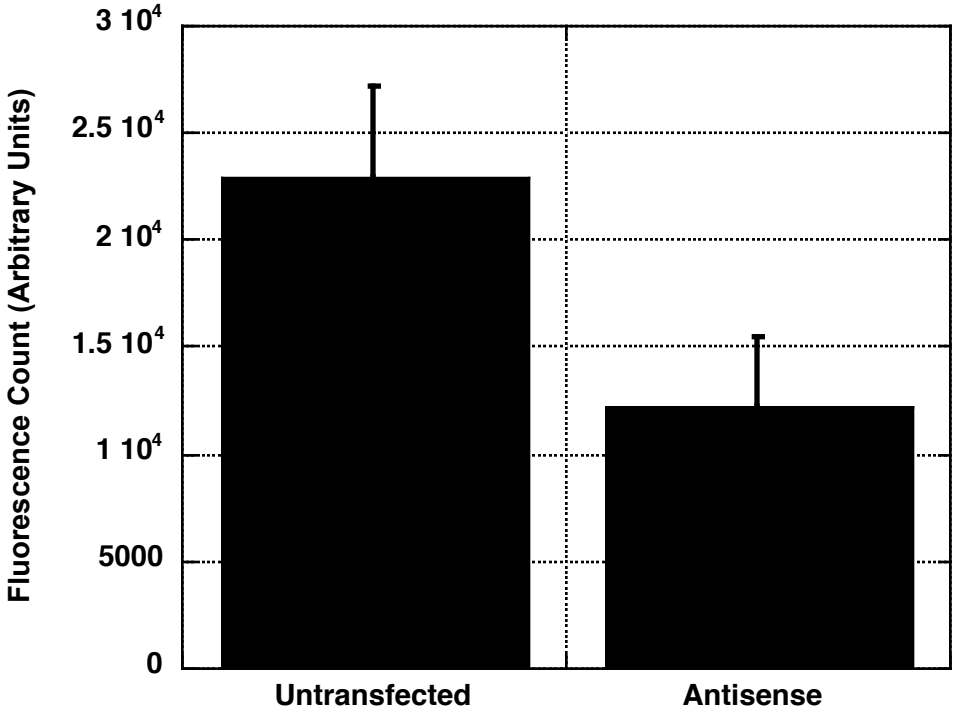

Figure 10: Suppression of ATPase II expression or activity causes an inhibition in APTL activity. B16F10 cells were transfected with mATPaseII antisense, mutant, and empty vectors. The cells transfected with the empty vector showed normal APTL activity for B16F10 cells, while the antisense constructs showed suppressed APTL activity.

Isolation and Analysis of Mouse ATPase II Promoter

The mouse genome has already been delineated (Nature, December 5, 2002), and also the coding sequence for the ATPase II gene and the organization of its exons are known. Since the mouse ATPase II promoter has not been studied, I started by identifying the positions of the exons on the mouse ATPase II gene. Both exons 1, and 2 were used as reference points to analyze the upstream sequences on mouse chromosome 5 (UCSC Genome Browser on Mouse Feb.2003 Freeze). Considering the fact that is partial homology has been observed between mouse and human ATPase II sequence, it is expected that the mouse ATPase II gene would also have a similar promoter sequence as seen in Figure 11. Using this information we were able to align the putative human ATPase II core promoter and get the putative mouse ATPase II core promoter. This sequence was also identified as a putative "core" promoter region (~200 bp) by the software PromoterInspector. Aside from this information, a relatively large (~12 kb) upstream segment was analyzed, in order to identify the putative full promoter sequence 5' of the translation start site. The activity of the putative promoter sequences was tested by ligating them into the luciferase reporter vector, pGL3Basic, and transfecting the recombinant constructs into four different mouse cell lines, as illustrated by Figure 12. The pattern of luciferase reporter activity remained consistent from cell line to cell line, however the reporter activity of the core promoter in the HN2 cell line was by far the highest. The putative core promoter sequence harbors many transcription factor-binding sites, which are summarized in **Table 3**. The region from position -318 to position +193 contains a large number of transcription factor binding sites and also sites selective for

the core promoter binding protein (CPBP), which is often observed in TATA-less promoters as illustrated by Figures 11 & 13 [Novina 1996].

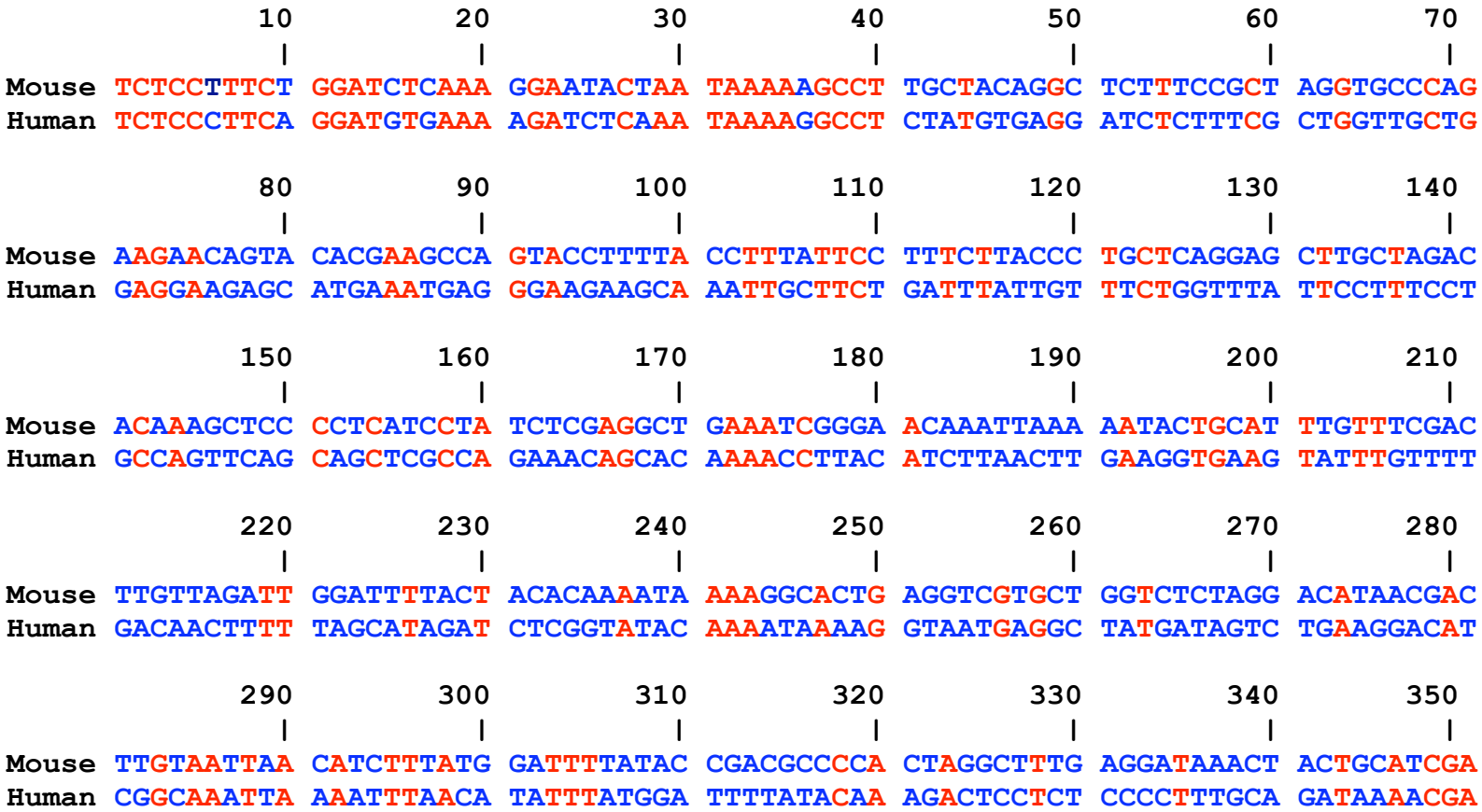

Figure 11: Comparative Analysis of Mouse ATPase II Promoter with Human ATPase II Promoter
The identical nucleotides are shown in red. The predicted putative core promoter is shown here from base 742 to 1252. The translation start site is shown here by the green at base 1303. Refer to Table 3 for transcription factor location. The Full/Distal forward primer runs from position 34 – 59 bp; Distal reverse runs from 761-739 bp; The core forward primer sits at the following position 742-768 bp and The core reverse sits at position 1262-1242bp, respectively.

```
                360         370         380         390         400         410         420
                  |           |           |           |           |           |           |
Mouse ACTTTCTGGA GCAGAAACCA CAAACAGCAT AATTTTTGCT TGGTTAACCA CGTGGTCAAC AGTTGGTTTG
Human CTGCATCCAA CTTTATGCAG ATTTAACTAA AAGAAAAAAA AAAAGTCTTT TGTGAACCAC CTGGGCCAAT

                430         440         450         460         470         480         490
                  |           |           |           |           |           |           |
Mouse GTTGCAGTTT CAGAGCCTTA ACAGGTTGCA GAGGACGAAC TGGTGGGAAG TACGGGCTCA CACACCCACG
Human ACTTAGTTGG CTTAATTGCT ATTTCAGTGC CTTGTCAGGC TGCAGAGCCT GAACTAGGGA GATGCACCGG

                500         510         520         530         540         550         560
                  |           |           |           |           |           |           |
Mouse CAGGTTGTGT GGCTGGAAGC CTTAAAACGA CAAGAGGAAC CGTTCCAGTG GCTTCAGGTC TCACAGCCTG
Human GCCCACTTGC AGGCGGGGCC CAGATGCACC CAAGCCCCAT GGACAAGAGC ACCATGGGCA CCAGGGGCCT

                570         580         590         600         610         620         630
                  |           |           |           |           |           |           |
Mouse CTACTACAGA GGGTTCACGT TCATCTCAGG CCAGGAGTCA GGCTGGGTGT TGAGATAGGC TAGGATTCCA
Human CCCGACCTGG CAGCCTGTTG CTAGTGGGCG AGGCAGGAGG ACAAGTGCGG CTCAGGCCAC GAGTCGGGCT

                640         650         660         670         680         690         700
                  |           |           |           |           |           |           |
Mouse CTCAGAGGGC GAATGCAGGG TCCCCCCACA TCAGCAGAGA CGTCACCCAC AGAGTCTCAG AGGCTTAGAC
Human GGGCGTGCAG AGAGGTTAGA ATTACACCCA GATGGCGAAC AGTCAGTCGT TCCTTTCCTG CTCTGGCTGG

                710         720         730         740         750         760         770
                  |           |           |           |           |           |           |
Mouse TCAAGCTGCC CACACCGAAC CCAACACCCT GGCGCTGAGG ACGGTCGGTT CTATCGCATT GTAGAGCCAG
Human GAGCTAAACC TTGTAGTCCC AGACCCTTTC GCCTTCGCCT GCCGGCTCAG ACCCAACAGC TCTTTCCGGA
```

Figure 11 (Continued)

```
              780         790         800         810         820         830         840
                |           |           |           |           |           |           |
Mouse AAGGTGGCTG TAGGGGATGC CAGAGCTTTC AGAGCTAAAG AAGCTCTTCC TCTTTTATTA AGGCTTGGGA
Human CGACGGGCGG CTCCACTGCG ATCAAAAGCC AGGGGTAGCG GGAGGGGATT CGTGAGAATG CAGCAGCCAG

              850         860         870         880         890         900         910
                |           |           |           |           |           |           |
Mouse CACTTGTACT GGCCTCAAGG AGGGCCGAGG TGGGCCGAGA AGCCGAGAAT GCTAGATCGA AGTCCCCTCC
Human AGCAGTCTTT CCTTTCTGAG CAAGATGTGA GAGAGTCCGA GTGGCCTGGA GGAGGAACCG GGTCAACCAA

              920         930         940         950         960         970         980
                |           |           |           |           |           |           |
Mouse CCGCGGATGG TACGGTCCGA ACTGGGCGGG ACCTGGAGGC TCGGCGGCCC TGTCCCCGCC CCACTCCAGG
Human CTCCACAGGG CGGAGCGAAA ACGCTGGAGG ACTAAGGAGG CTAAGAGTTG ATCCCCCCTT TGAGTCGTGA

              990         1000        1010        1020        1030        1040        1050
                |           |           |           |           |           |           |
Mouse AGGCCAGCGA GTGAGCGCGC GCCCCGCAGA CCCCGCCCCC GGCGCCGTCC CCGGCTCCGC CCCTCGAGCC
Human TACGGTCCGA AGCGGGGCGG GGCGGGGCGA AGGAGGCTCC CCCTGGCTCT CCCCGCCCCT CACCCGCCTT

              1060        1070        1080        1090        1100        1110        1120
                |           |           |           |           |           |           |
Mouse CGCTCCTCTG CCACTGCGGG GAGACCTAGG CGGCTCTGCG GACGCAGCTC CTTCGCCGCC TTCCCCCTCC
Human CCTTGCTGAG CGGCCGCGGG AGGGGGAGCG CGAGCCCCGC AGGCCCCTCC CCCGGCGCCG GCGCCCGAGC

              1130        1140        1150        1160        1170        1180        1190
                |           |           |           |           |           |           |
Mouse CGTCCAGTGC CCAGGCGGCT CCTGGCGGCG ACGCTGCCCT GGGTGGGAGG CGCGGCCCCG CGGCAGCTGA
Human TCCGCCCCTC GCCGAGCCGC CCCTCCGCGG CTGCAGCAAG AGCTCGCCCA GCTCTGCGGG CGCCGCCACC
```

Figure 11 (Continued)

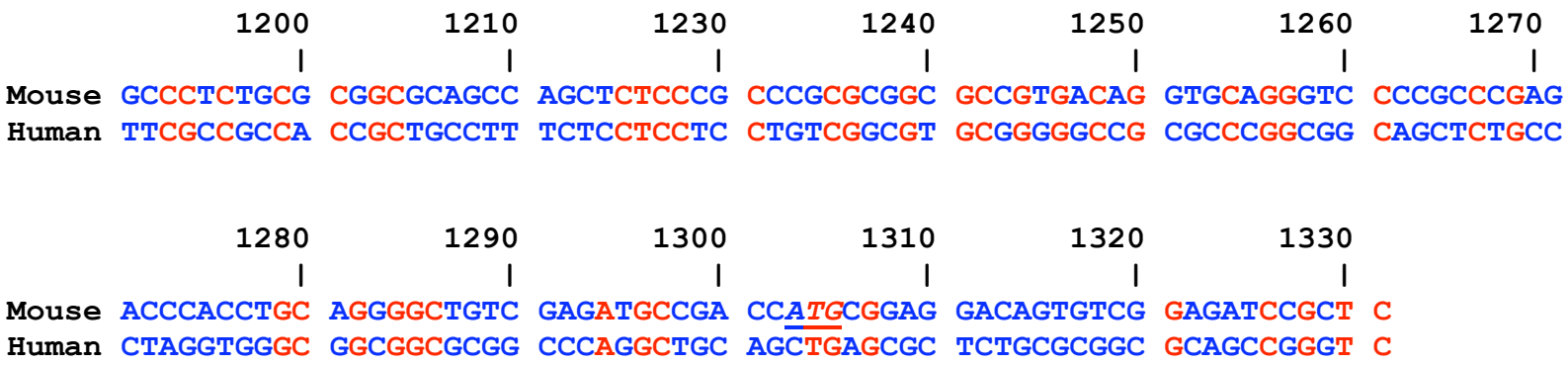

Figure 11 (Continued)

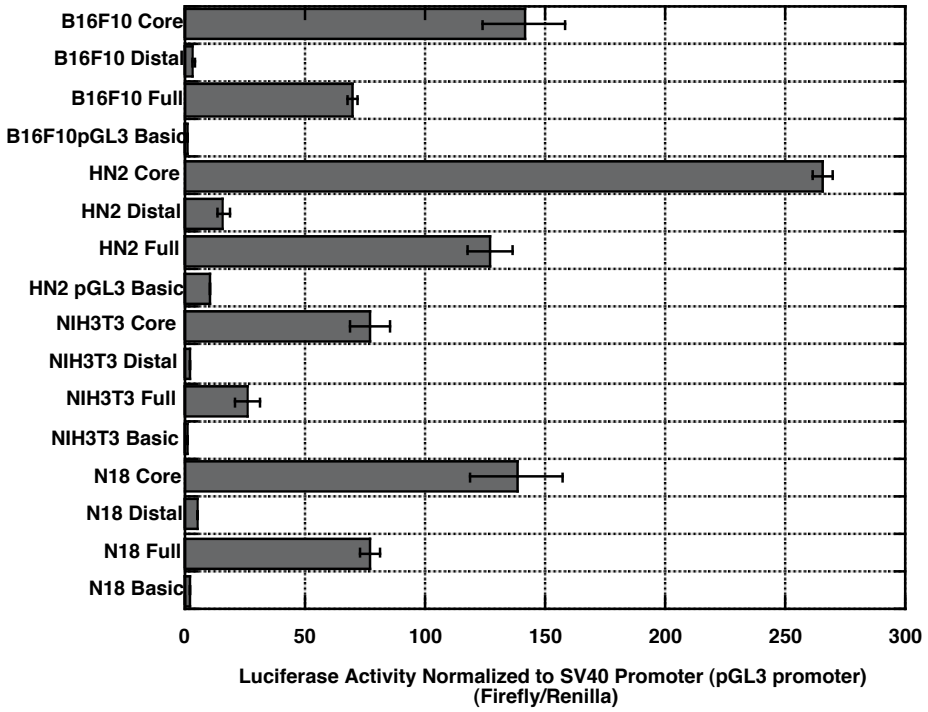

Figure 12: Transcriptional Activity of the Mouse ATPase II Promoter
The 1.5-kb promoter of the *ATPase II* gene has been studied in multiple cell lines, and this promoter appears to be almost equally active in neural and non-neural cell types. These cells were transfected with the full, distal and core promoters. pRL-TK was used as an internal control. Cells were grown in triplicate to 30% confluence in 24-well plates and then transfected each DNA vector using Effectene reagent (Qiagen). After 48 h the cells were lysed and assayed for firefly luciferase activity using a kit from Promega. The activity of the ATPase II promoter and parts of it is expressed as a ratio of firefly luciferase to renilla luciferase activity of each cell lysate

```
            -1020       -1010       -1000       -990        -980        -970
              |           |           |           |           |           |
Cons_seq AAAGCCTTGC TACAGGCTCT TTCCGCTAGG TGCCCAGAAG AACAGTACAC GAAGCCAGTA
Full     AAAGCCTTGC TACAGGCTCT TTCCGCTAGG TGCCCAGAAG AACAGTACAC GAAGCCAGTA
Distal   AAAGCCTTGC TACAGGCTCT TTCCGCTAGG TGCCCAGAAG AACAGTACAC GAAGCCAGTA
Core     ---------- ---------- ---------- ---------- ---------- ----------

            -960        -950        -940        -930        -920        -910
              |           |           |           |           |           |
Cons_seq CCTTTTACCT TTATTCCTTT CTTACCCTGC TCAGGAGCTT GCTAGACACA AAGCTCCCCT
Full     CCTTTTACCT TTATTCCTTT CTTACCCTGC TCAGGAGCTT GCTAGACACA AAGCTCCCCT
Distal   CCTTTTACCT TTATTCCTTT CTTACCCTGC TCAGGAGCTT GCTGGACACA AAGCTCCCCT
Core     ---------- ---------- ---------- ---------- ---------- ----------

            -900        -890        -880        -870        -860        -850
              |           |           |           |           |           |
Cons_seq CATCCTATCT CGAGGCTGAA ATCGGGAACA AATTAAAAAT ACTGCATTTG TTTCGACTTG
Full     CATCCTATCT CGAGGCTGAA ATCGGGAACA AATTAAAAAT ACTGCATTTG TTTCGACTTG
Distal   CATCCTATCT CGAGGCTGAA ATCGGGAACA AATTAAAAAT ACTGCATTTG TTTCGACTTG
Core     ---------- ---------- ---------- ---------- ---------- ----------
```

Figure 13: Isolation and Characterization of the *ATPaseII* promoter.
Shown here is the Sequence alignment of the promoter constructs prepared and used in Figure 11. The constructs were manually aligned using sequencing data obtained from ACGT, Inc and the promoter variant obtained from the UCSC genome browswer. Bold, Italicized and underlined regions at the beginning of the sequence is the Forward primer for both full and distal promoters.

```
            -840       -830       -820       -810       -800       -790
              |          |          |          |          |          |
Cons_seq TTAGATTGGA TTTTACTACA CAAAATAAAA GGCACTGAGG TCGTGCTGGT CTCTAGGACA
Full     TTAGATTGGA TTTTACTACA CAAAATAAAA GGCACTGAGG TCGTGCTGGT CTCTAGGACA
Distal   TTAGATTGGA TTTTACTACA CAAAATAAAA GGGACTGAGG TCGTGCTGGT CTCTAGGACA
Core     ---------- ---------- ---------- ---------- ---------- ----------

            -780       -770       -760       -750       -740       -730
              |          |          |          |          |          |
Cons_seq TAACGACTTG TAATTAACAT CTTTATGGAT TTTATACCGA CGCCCCACTA GGCTTTGAGG
Full     TAACGACTTG TAATTAACAT CTTTATGGAT TTTATACCGA CGCCCCACTA GGCTTTGAGG
Distal   TAACGACTTG TAATTAACAT CTTTATGGAT TTTATACCGA CGCCCCACTA GGCTTTGAGG
Core     ---------- ---------- ---------- ---------- ---------- ----------

            -720       -710       -700       -690       -680       -670
              |          |          |          |          |          |
Cons_seq ATAAACTACT GCATCGAACT TTCTGGAGCA GAAACCACAA ACAGCATAAT TTTTGCTTGG
Full     ATAAACTACT GCATCGAACT TTCTGGAGCA GAAACCACAA ACAGCATAAT TTTTGCTTGG
Distal   ATAAACTACT GCATCGAACT TTCTGGAGCA GAAACCACAA ACAGCATAAT TTTTGCTTGG
Core     ---------- ---------- ---------- ---------- ---------- ----------

            -660       -650       -640       -630       -620       -610
              |          |          |          |          |          |
Cons_seq TTAACCACGT GGTCAACAGT TGGTTTGGTT GCAGTTTCAG AGCCTTAACA GGTTGCAGAG
Full     TTAACCACGT GGTCAACAGT TGGTTTGGTT GCAGTTTCAG AGCCTTAACA GGTTGCAGAG
Distal   TTAACCACGT GGTCAACAGT TGGTTTGGTT GCAGTTTCAG AGCCTTAACA GGTTGCAGAG
Core     ---------- ---------- ---------- ---------- ---------- ----------
```

Figure 13 (Continued)

```
            -600        -590        -580        -570        -560        -550
              |           |           |           |           |           |
Cons_seq GACGAACTGG TGGGAAGTAC GGACTCACAC ACCCACGCAG GTTGTGTGGC TGGAAGCCTT
Full     GACGAACTGG TGGGAAGTAC GGACTCACAC ACCCACGCAG GTTGTGTGGC TGGAAGCCTT
Distal   GACGAACTGG TGGGAAGTAC GGGCTCACAC ACCCACGCAG GTTGTGTGGC TGGAAGCCTT
Core     ---------- ---------- ---------- ---------- ---------- ----------

            -540        -530        -520        -510        -500        -490
              |           |           |           |           |           |
Cons_seq AAAACGACAA GAGGAACCGT TCCAGTGGCT TCAGGTCTCA CAGCCTGCTA CTACAGAGGG
Full     AAAACGACAA GAGGAACCGT TCCAGTGGCT TCAGGTCTCA CAGCCTGCTA CTACAGAGGG
Distal   AAAACGACAA GAGGAACCGT TCCAGTGGCT TCAGGTCTCA CAGCCTGCTA CTACAGAGGG
Core     ---------- ---------- ---------- ---------- ---------- ----------

            -480        -470        -460        -450        -440        -430
              |           |           |           |           |           |
Cons_seq TTCACGTTCA TCTCAGGCCA GGAGTCAGGC TGGGTGTTGA GATAGGCTAG GATTCCACTC
Full     TTCACGTTCA TCTCAGGCCA GGAGTCAGGC TGGGTGTTGA GATAGGCTAG GATTCCACTC
Distal   TTCACGTTCA TCTCAGGCCA GGAGTCAGGC TGGGTGTTGA GATAGGCTAG GATTCCACTC
Core     ---------- ---------- ---------- ---------- ---------- ----------

            -420        -410        -400        -390        -380        -370
              |           |           |           |           |           |
Cons_seq AGAGGGCGAA TGCAGGGTCC CCCCACATCA GCAGAGACGT CACCCACAGA GTCTCAGAGG
Full     AGAGGGCGAA TGCAGGGTCC CCCCACATCA GCGGAGACGT CACCCACAGA GTCTCAGAGG
Distal   AGAGGGCGAA TGCAGGGTCC CCCCACATCA GCAGAGACGT CACCCACAGA GTCTCAGAGG
Core     ---------- ---------- ---------- ---------- ---------- ----------
```

Figure 13 (Continued)

```
            -360        -350        -340        -330        -320        -310
              |           |           |           |           |           |
Cons_seq CTTAGACTCA AGCTGCCCAC ACCGAACCCA ACACCCTGGC GCTGAGGACG GTCGGTTCTA
Full     CTTAGACTCA AGCTGCCCAC ACCGAACCCA ACACCCTGGC GCTGAGGACG GTCGGTTCTA
Distal   CTTAGACTCA AGCTGCCCAC ACCGAACCCA ACACCCTGGC GCTGAGGACG GTCGGTTCTA
Core     ---------- ---------- ---------- ---------- --------CG GTCGGTTCTA

            -300        -290        -280        -270        -260        -250
              |           |           |           |           |           |
Cons_seq TCGCATTGTA GAGCCAGAAG GTGGCTGTAG GGGATGCCAG AGCTTTCAGA GCTAAAGAAG
Full     TCGCATTGTA GAGCCAGAAG GTGGCTGTAG GGGATGCCAG AGCTTTCAGA GCTAAAGAAG
Distal   TCGCATTG-- ---------- ---------- ---------- ---------- ----------
Core     TCGCATTGTA GAGCCAGAAG GTGGCTGTAG GGGATGCCAG AGCTTTCAGA GCTAAAGAAG

            -240        -230        -220        -210        -200        -190
              |           |           |           |           |           |
Cons_seq CTCTTCCTCT TTTATTAAGG CTTGGGACAC TTGTACTGGC CTCAAGGAGG GCCGAGGTGG
Full     CTCTTCCTCT TTTATTAAGG CTTGGGACAC TTGTACTGGC CTCAAGGAGG GCCAAAGTGG
Distal   ---------- ---------- ---------- ---------- ---------- ----------
Core     CTCTTCCTCT TTTATTAAGG CTTGGGACAC TTGTACTGGC CTCAAGGAGG GCCGAGGTGG

            -180        -170        -160        -150        -140        -130
              |           |           |           |           |           |
Cons_seq GCCGAGAAGC CGAGAATGCT AGATCGAAGT CCCCTCCCCG CGGATGGTAC GGTCCGAACT
Full     GCCGAGAAGC CGAGAATGCT AGATCGAAGT CCCCTCCCCG CGGATGGTAC GGTCCGAACT
Distal   ---------- ---------- ---------- ---------- ---------- ----------
Core     GCCGAGAAGC CGAGATTGCT AGATCGAAGT CCCCTCCCCG CGGATGTTAC GTTCCGAACT
```

Figure 13 (Continued)

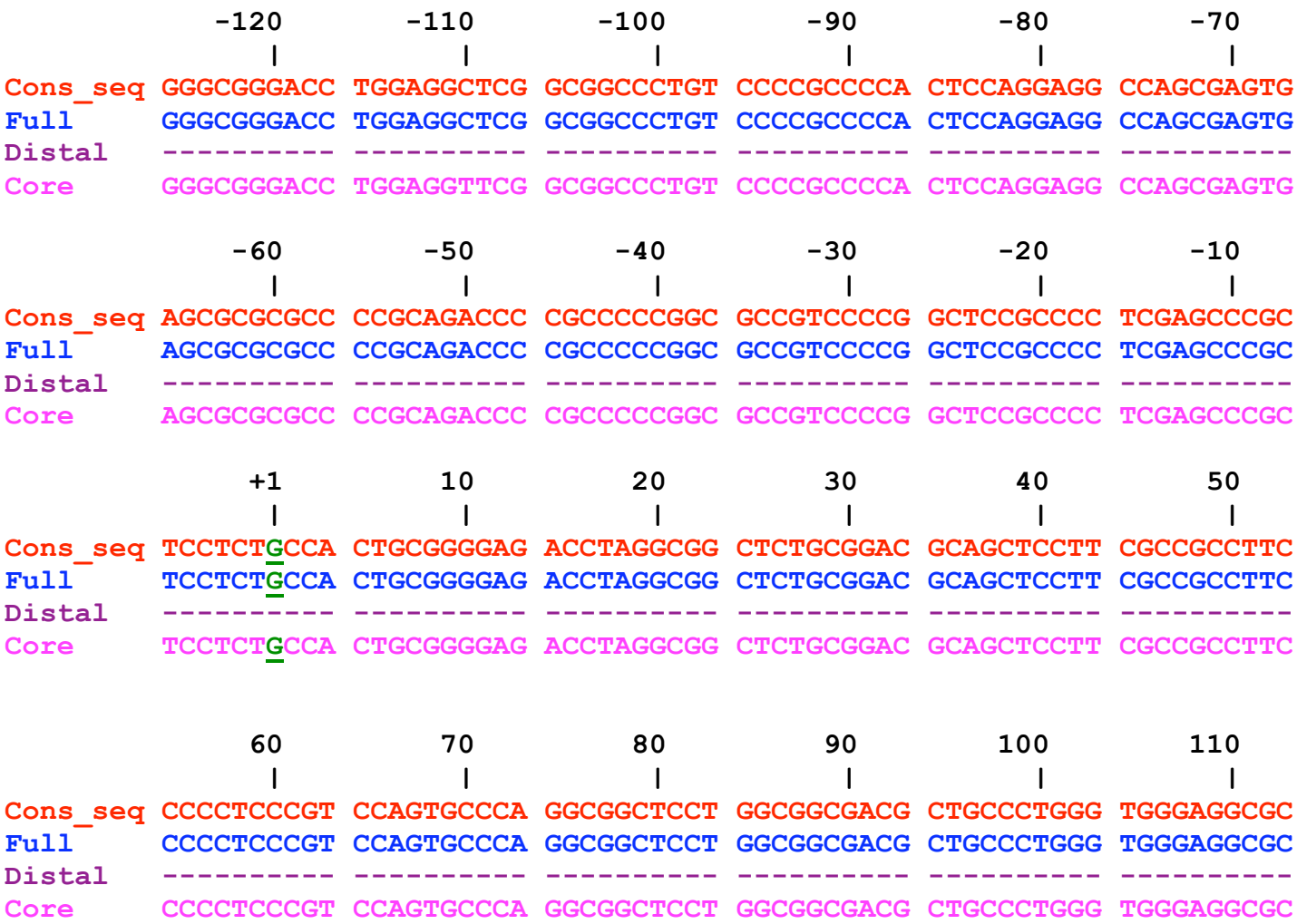

Figure 13 (Continued)

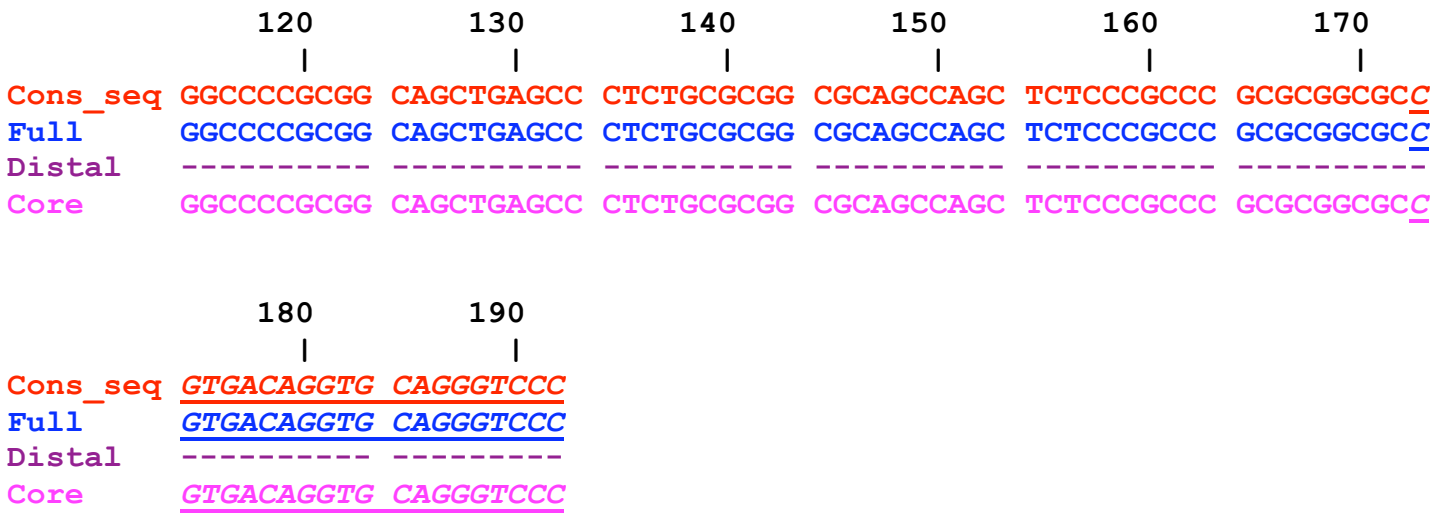

Figure 13 (Continued)

Table 3: Transcription Factor Binding sites present in the Mouse ATPase II putative 'Core Promoter'

Transcription Factor	Further Information	Position	Strand	Core Sequence	Full Sequence
ZID.01	Zinc Finger with interaction domain	-303 to -291	(-)	GCTC	tgGCTCtacaatg
CP2.02	LBP-1c (leader binding protein-1c), LSF (Late SV40 factor), CP2, SEF (SAA3 enhancer factor)	-296 to -278	(-)	ACAG	tACAGccaccttctggctc
NFKappaB50.01	NF-KappaB (p50)	-279 to -265	(+)	GGGG	taGGGGatgccagag
ZBRK1.01	Transcription factor with 8 central zinc fingers and an N-terminal KRAB domain	-278 to -254	(+)	CCAG	aggggatgCCAGagctttcagagct
MYT1L.01	Myelin transcription factor 1-like, neuronal C2HC zinc finger factor	-271 to -259	(-)	AGCT	tgaaAGCTctggc
ELF2.01	Ets –family member ELF-2 (NERF1a)	-250 to -234	(-)	GGAA	aaaagaGGAAgagcttc
TATA.02	Mammalian C-type LTR TATA box	-244 to -228	(-)	TAAA	cttaaTAAAagaggaag
CDX1.01	Intestine specific homeodomain factor CDX-1	-243 to -225	(+)	TTTA	ttcctctTTTAttaaggct
HOXC13.01	Homeodomain transcription factor HOXC13	-240 to -224	(-)	TAAA	aagccttaaTAAAagag
NKX25.02	Homeo domain factor Nkx-2.5/Csx, tinman homolog low affinity sites	-239 to -227	(-)	TAAT	cctTAATaaaaga

Table 3 (Continued)

Transcription Factor	Further Information	Position	Strand	Core Sequence	Full Sequence
PAX3.01	Pax-3 paired domain protein, expressed in embryogenesis, mutations correlate to Waardenburg Syndrome	-194 to -182	(-)	TCGG	TCGGcccacctcg
CKROX.01	Collagen Krox Protein (zinc finger protein 67-zfp67)	-159 to -143	(-)	GGGA	tccgcgGGGAggggact
MAX.01	Myc associated zinc finger protein (MAZ)	-159 to -147	(-)	GAGG	cgggGAGGgact
SP1.01	Stimulating protein 1 SP1, ubiquitous zinc finger transcription factor	-159 to -145	(-)	GGAG	cgcggGGAGgggact
MZF1.01	Myeloid zinc finger protein MZF1	-157 to -151	(-)	GGGG	gaGGGGa
MAZ.01	Myc associated zinc finger protein (MAZ)	-154 to -142	(-)	GCGG	atccGCGGggagg
DMP1.01	Cyclin D-interacting myb-like protein, DMTF1-cyclin D Binding myb-like transcription factor 1	-150 to -138	(+)	GGAT	cccgcGGATggta

Table 3 (Continued)

Transcription Factor	Further Information	Position	Strand	Core Sequence	Full Sequence
SP2.01	Sp2, member of the Sp.XKLF transcription factors with three C2H2 zinc fingers in a conserved carboxyl terminal domain	-130 to -116	(+)	GGAC	aactgggcgGGACct
BNC.01	Basonuclin, cooperates with USF1 in rDNA PolI transcription	-109 to -91	(+)	TGTC	tcggcggcccTGTCcccgc
ZF9.01	Core promoter-binding protein (CPBP) with 3 Krueppel-type zinc fingers	-102 to -79	(+)	CCGC	cctgtccCCGCcccactccagga
MAZR.01	MYC-associated zinc finger protein related transcription factor	-99 to -87	(-)	GGGG	tggggcGGGGaca
SP1.01	Stimulating protein SP1, ubiquitous zinc finger transcription factor	-99 to -85	(-)	GGCG	agtggGGCGgggaca
MZF1.01	Myeloid zinc finger protein MZF1	-97 to -92	(-)	GGGG	gcGGGGa
MUSCLE_INI.01	Muscle Initiator Sequence	-95 to -77	(+)	CCAC	cccgccCCACtccaggagg
EBVR.01	Epstein-Barr virus transcription factor R	-93 to -73	(-)	GGGG	ctggcctcctggagtGGGGcg
WT1.01	Wilms Tumor Suppressor	-73 to -57	(+)	TGAG	gcgagTGAGcgcgcgcc

Table 3 (Continued)

Transcription Factor	Further Information	Position	Strand	Core Sequence	Full Sequence
NRF1.01	Nuclear respiratory factor 1 (NRF1), bZIP transcription factor that acts on nuclear genes encoding mitochondrial proteins	-71 to -56	(-)	GCGC	gggGCGCgcgctcactc
ZF5.01	Zinc Finger/POZ domain transcription	-69 to -59	(+)	GCGC	gtgaGCGCgcg
CDE.01	Cell cycle-dependent element, CDF-1 binding site (CDE/CHR tandem elements regulate cell cycle dependent repression)	-68 to -55	(-)	CGCG	ggggCGCGcgctc
ZNF76_143.01	ZNF143 is the human ortholog of Xenopus Staf, ZNF76 is a DNA binding protein related to ZNF143 and Staf	-62 to -40	(+)	CCCC	cgcgCCCCgcagaccccgccccc
EGR1.02	EGR1, early growth response 1	-50 to -34	(-)	GGGC	ggcgccggGGGCgggggt
PLAG1.01	Pleomorphic adenoma gene (PLAG) 1, a developmentally regulated C2H2 zinc finger protein	-35 to -15	(-)	GAGG	GAGGggcggagccggggacgg
GC.01	GC box elements	-28 to -14	(-)	GGCG	cgaggGGCGgagccg

Table 3 (Continued)

Transcription Factor	Further Information	Position	Strand	Core Sequence	Full Sequence
ATF6.01	Member of b-zip family, induced by ER damage/stress, binds to the ERSE in association with NF-Y	-1 to +13	(+)	CCAC	ctgCCACtgcgggga
TAXCREB.02	Tax/CREB complex	+25 to +45	(+)	GGAC	ctctgcGGACgcagctccttc
PAX5.01	B-cell-specific activating protein	+82 to +110	(-)	CCCA	ctcccaCCCAgggcagcgtcgcccgccagg
WHN.01	Winged helix protein, involved in hair keratinization and thymus epithelium differentiation	+89 to +99	(+)	ACGC	gcgACGCtgcc
NGFIC.01	Nerve growth factor-induced protein C	+98 to +114	(+)	GGGT	ccctGGGTgggaggcgc
AP2.01	Activator Protein 2	+115 to +127	(+)	CCCC	ggCCCCgcggcag
AP4.01	Activator Protein 4	+119 to +135	(-)	CAGC	gggctCAGCtgccgcgg
AREB6.03	AREB6 (Atp1a1 regulatory element binding factor 6)	+176 to +188	(-)	CACC	cctgCACCtgtca

Deletion Analysis of Mouse ATPase II Promoter

The sequence termed as core promoter, started at position -318 and stretched up to position +193 with respect to the transcription start site. This fragment yielded a higher activity than that of the full promoter. Further deletion of the core promoter to -270 to +33 resulted in a sharp drop in activity in all the cell lines tested in the above assay (Figure 15). We did observe varying cell type specificity with each of the fragments (Figure 14 & 15). For example, the -119 fragment showed low activity in all cells except in the NIH3T3 cells.

Table 4: Transcription Factor binding sites harbored on the Deletion fragments of the Mouse ATPase II Core Promoter – refer to Table 3 for detailed description of transcription factors

Promoter Fragment	Transcription Factor Binding Sites
-318	ZID, CP2, NFKappaB, ZBRK1, MYT1, ELF2, TATA, CDX1, HOXC13, NKX25, PAX3, CKROX, MAX, SP1, MZF1, MAZ, DMP1, SP2, BNC, ZF9, MAZR, MUSCLE_INI, EBVR, WT1, NRF1, ZF5, CDE, ZNF76_143, EGR1, PLAG1, GC, ATF6, TAXCREB, PAX5, WHN, NGFIC, AP2, AP4, AREB6
-270	MYT1, ELF2, TATA, CDX1, HOXC13, NKX25, PAX3, CKROX, MAX, SP1, MZF1, MAZ, DMP1, SP2, BNC, ZF9, MAZR, MUSCLE_INI, EBVR, WT1, NRF1, ZF5, CDE, ZNF76_143, EGR1, PLAG1, GC, ATF6, TAXCREB, PAX5, WHN, NGFIC, AP2, AP4, AREB6
-218	PAX3, CKROX, MAX, SP1, MZF1, MAZ, DMP1, SP2, BNC, ZF9, MAZR, MUSCLE_INI, EBVR, WT1, NRF1, ZF5, CDE, ZNF76_143, EGR1, PLAG1, GC, ATF6, TAXCREB, PAX5, WHN, NGFIC, AP2, AP4, AREB6
-172	CKROX, MAX, SP1, MZF1, MAZ, DMP1, SP2, BNC, ZF9, MAZR, MUSCLE_INI, EBVR, WT1, NRF1, ZF5, CDE, ZNF76_143, EGR1, PLAG1, GC, ATF6, TAXCREB, PAX5, WHN, NGFIC, AP2, AP4, AREB6
-119	BNC, ZF9, MAZR, MUSCLE_INI, EBVR, WT1, NRF1, ZF5, CDE, ZNF76_143, EGR1, PLAG1, GC, ATF6, TAXCREB, PAX5, WHN, NGFIC, AP2, AP4, AREB6
-70	ZF5, CDE, ZNF76_143, EGR1, PLAG1, GC, ATF6, TAXCREB, PAX5, WHN, NGFIC, AP2, AP4, AREB6
-13	ATF6, TAXCREB, PAX5, WHN, NGFIC, AP2, AP4, AREB6
+33	TAXCREB, PAX5, WHN, NGFIC, AP2, AP4, AREB6

```
                -310        -300        -290        -280
                  |           |           |           |
Cons_Seq CGGTCGGTTC TATCGCATTG TAGAGCCAGA AGGTGGCTGT
CoreProm CGGTCGGTTC TATCGCATTG TAGAGCCAGA AGGTGGCTGT

                -270        -260        -250        -240
                  |           |           |           |
Cons_Seq AGGGGATGCC AGAGCTTTCA GAGCTAAAGA AGCTCTTCCT
CoreProm AGGGGATGCC AGAGCTTTCA GAGCTAAAGA AGCTCTTCCT
Del_1       CC AGAGCTTTCA GAGCTAAAGA AGCTCTTCCT

                -230        -220        -210        -200
                  |           |           |           |
Cons_Seq CTTTTATTAA GGCTTGGGAC ACTTGTACTG GCCTCAAGGA
CoreProm CTTTTATTAA GGCTTGGGAC ACTTGTACTG GCCTCAAGGA
Del_1    CTTTTATTAA GGCTTGGGAC ACTTGTACTG GCCTCAAGGA
Del_2                          ACTTGTACTG GCCTCAAGGA

                -190        -180        -170        -160
                  |           |           |           |
Cons_Seq GGGCCGAGGT GGGCCGAGAA GCCGAGAATG CTAGATCGAA
CoreProm GGGCCGAGGT GGGCCGAGAA GCCGAGAATG CTAGATCGAA
Del_1    GGGCCGAGGT GGGCCGAGAA GCCGAGAATG CTAGATCGAA
Del_2    GGGCCGAGGT GGGCCGAGAA GCCGAGAATG CTAGATCGAA
Del_3                                AATG CTAGATCGAA

                -150        -140        -130        -120
                  |           |           |           |
Cons_Seq GTCCCCTCCC CGCGGATGGT ACGGTCCGAA CTGGGCGGGA
CoreProm GTCCCCTCCC CGCGGATGGT ACGGTCCGAA CTGGGCGGGA
Del_1    GTCCCCTCCC CGCGGATGGT ACGGTCCGAA CTGGGCGGGA
Del_2    GTCCCCTCCC CGCGGATGGT ACGGTCCGAA CTGGGCGGGA
Del_3    GTCCCCTCCC CGCGGATGGT ACGGTCCGAA CTGGGCGGGA
Del_4                                              A
```

Figure 14: Isolation and Characterization of the mouse *ATPase II* putative 'Core' promoter.

Shown here is the sequence alignment of the Deletion constructs prepared and used in Figure 15. Sequences were aligned and compared using data obtained from sequencing. The main sequence referred to here is the sequence obtained from the database (UCSC genome browser), which was confirmed by PromoterInspector to be the putative mouse "core promoter". The italicized/underlined regions indicate the primers used to generate the deletion fragments of the core promoter.

```
                -110        -100         -90         -80
                  |           |           |           |
Cons_Seq  CCTGGAGGCT CGGCGGCCCT GTCCCCGCCC CACTCCAGGA
CoreProm  CCTGGAGGCT CGGCGGCCCT GTCCCCGCCC CACTCCAGGA
Del_1     CCTGGAGGCT CGGCGGCCCT GTCCCCGCCC CACTCCAGGA
Del_2     CCTGGAGGCT CGGCGGCCCT GTCCCCGCCC CACTCCAGGA
Del_3     CCTGGAGGCT CGGCGGCCCT GTCCCCGCCC CACTCCAGGA
Del_4     CCTGGAGGCT CGGCGGCCCT GTCCCCGCCC CACTCCAGGA

                -70         -60         -50         -40
                  |           |           |           |
Cons_Seq  GGCCAGCGAG TGAGCGCGCG CCCCGCAGAC CCCGCCCCCG
CoreProm  GGCCAGCGAG TGAGCGCGCG CCCCGCAGAC CCCGCCCCCG
Del_1     GGCCAGCGAG TGAGCGCGCG CCCCGCAGAC CCCGCCCCCG
Del_2     GGCCGGCGAG TGAGCGCGCG CCCCGCAGAC CCCGCCCCCG
Del_3     GGCCAGCGAG TGAGCGCGCG CCCCGCAGAC CCCGCCCCCG
Del_4     GGCCAGCGAG TGAGCGCGCG CCCCGCAGAC CCCGCCCCCG
Del_5           AG TGAGCGCGCG CCCCGCAGAC CCCGCCCCCG

                -30         -20         -10          +1
                  |           |           |           |
Cons_Seq  GCGCCGTCCC CGGCTCCGCC CCTCGAGCCC GCTCCTCTGC
CoreProm  GCGCCGTCCC CGGCTCCGCC CCTCGAGCCC GCTCCTCTGC
Del_1     GCGCCGTCCC CGGCTCCGCC CCTCGAGCCC GCTCCTCTGC
Del_2     GCGCCGTCCC CGGCTCCGCC CCTCGAGCCC GCTCCTCTGC
Del_3     GCGCCGTCCC CGGCTCCGCC CCTCGAGCCC GCTCCTCTGC
Del_4     GCGCCGTCCC CGGCTCCGCC CCTCGAGCCC GCTCCTCTGC
Del_5     GCGCCGTCCC CGGCTCCGCC CCTCGAGCCC GCTCCTCTGC
Del_6                                AGCCC GCTCCTCTGC

                 10          20          30          40
                  |           |           |           |
Cons_Seq  CACTGCGGGG AGACCTAGGC GGCTCTGCGG ACGCAGCTCC
CoreProm  CACTGCGGGG AGACCTAGGC GGCTCTGCGG ACGCAGCTCC
Del_1     CACTGCGGGG AGACCTAGGC GGCTCTGCGG ACGCAGCTCC
Del_2     CACTGCGGGG AGACCTAGGC GGCTCTGCGG ACGCAGCTCC
Del_3     CACTGCGGGG AGACCTAGGC GGCTCTGCGG ACGCAGCTCC
Del_4     CACTGCGGGG AGACCTAGGC GGCTCTGCGG ACGCAGCTCC
Del_5     CACTGCGGGG AGACCTAGGC GGCTCTGCGG ACGCAGCTCC
Del_6     CACTGCGGGG AGACCTAGGC GGCTCTGCGG ACGCAGCTCC
Del_7                                     ACGCAGCTCC
```

Figure 14 (Continued)

```
                50          60          70          80
                 |           |           |           |
Cons_Seq TTCGCCGCCT TCCCCCTCCC GTCCAGTGCC CAGGCGGCTC
CoreProm TTCGCCGCCT TCCCCCTCCC GTCCAGTGCC CAGGCGGCTC
Del_1    TTCGCCGCCT TCCCCCTCCC GTCCAGTGCC CAGGCGGCTC
Del_2    TTCGCCGCCT TCCCCCTCCC GTCCAGTGCC CAGGCGGCTC
Del_3    TTCGCCGCCT TCCCCCTCCC GTCCAGTGCC CAGGCGGCTC
Del_4    TTCGCCGCCT TCCCCCTCCC GTCCAGTGCC CAGGCGGCTC
Del_5    TTCGCCGCCT TCCCCCTCCC GTCCAGTGCC CAGGCGGCTC
Del_6    TTCGCCGCCT TCCCCCTCCC GTCCAGTGCC CAGGCGGCTC
Del_7    TTCGCCGCCT TCCCCCTCCC GTCCAGTGCC CAGGCGGCTC

                90         100         110         120
                 |           |           |           |
Cons_Seq CTGGCGGCGA CGCTGCCCTG GGTGGGAGGC GCGGCCCCGC
CoreProm CTGGCGGCGA CGCTGCCCTG GGTGGGAGGC GCGGCCCCGC
Del_1    CTGGCGGCGA CGCTGCCCTG GGTGGGAGGC GCGGCCCCGC
Del_2    CTGGCGGCGA CGCTGCCCTG GGTGGGAGGC GCGGCCCCGC
Del_3    CTGGCGGCGA CGCTGCCCTG GGTGGGAGGC GCGGCCCCGC
Del_4    CTGGCGGCGA CGCTGCCCTG GGTGGGAGGC GCGGCCCCGC
Del_5    CTGGCGGCGA CGCTGCCCTG GGTGGGAGGC GCGGCCCCGC
Del_6    CTGGCGGCGA CGCTGCCCTG GGTGGGAGGC GCGGCCCCGC
Del_7    CTGGCGGCGA CGCTGCCCTG GGTGGGAGGC GCGGCCCCGC

               130         140         150         160
                 |           |           |           |
Cons_Seq GGCAGCTGAG CCCTCTGCGC GGCGCAGCCA GCTCTCCCGC
CoreProm GGCAGCTGAG CCCTCTGCGC GGCGCAGCCA GCTCTCCCGC
Del_1    GGCAGCTGAG CCCTCTGCGC GGCGCAGCCA GCTCTCCCGC
Del_2    GGCAGCTGAG CCCTCTGCGC GGCGCAGCCA GCTCTCCCGC
Del_3    GGCAGCTGAG CCCTCTGCGC GGCGCAGCCA GCTCTCCCGC
Del_4    GGCAGCTGAG CCCTCTGCGC GGCGCAGCCA GCTCTCCCGC
Del_5    GGCAGCTGAG CCCTCTGCGC GGCGCAGCCA GCTCTCCCGC
Del_6    GGCAGCTGAG CCCTCTGCGC GGCGCAGCCA GCTCTCCCGC
Del_7    GGCAGCTGAG CCCTCTGCGC GGCGCAGCCA GCTCTCCCGC
```

Figure 14 (Continued)

```
                170         180         190
                  |           |           |
Cons_Seq CCGCGCGGCG CCGTGACAGG TGCAGGGTCC C
CoreProm CCGCGCGGCG CCGTGACAGG T--------- -
Del_1    CCGCGCGGCG CCGTGACAGG T--------- -
Del_2    CCGCGCGGCG CCGTGACAGG T--------- -
Del_3    CCGCGCGGCG CCGTGACAGG T--------- -
Del_4    CCGCGCGGCG CCGTGACAGG T--------- -
Del_5    CCGCGCGGCG CCGTGACAGG T--------- -
Del_6    CCGCGCGGCG CCGTGACAGG T--------- -
Del_7    CCGCGCGGCG CCGTGACAGG T--------- -
```

Figure 14 (Continued)

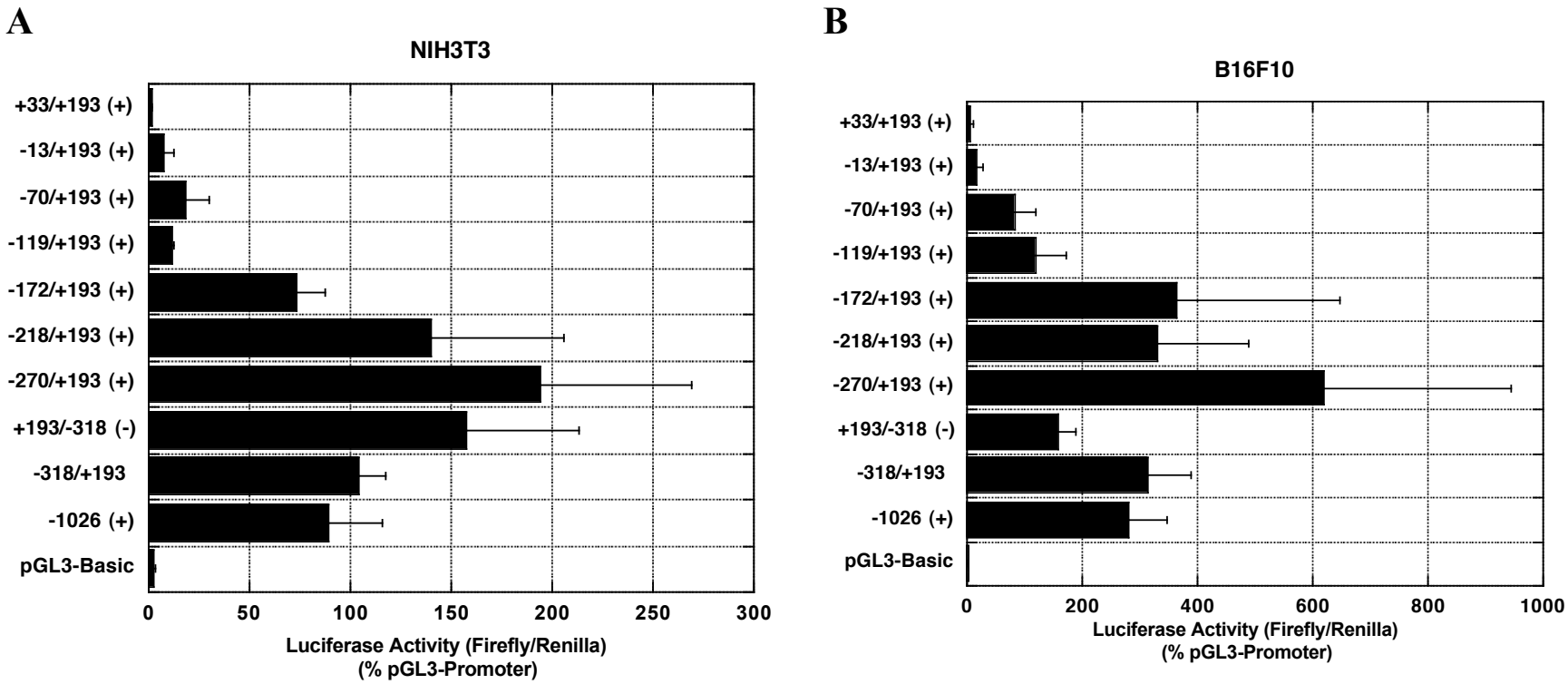

Figure 15 A-E: Deletion Analysis of the *ATPase II* promoter

Luciferase Activity of the promoter constructs transfected into Five different mouse cell lines – SN48 (Septal neuronal cells), B16F10 (melanomal cells), HN2 (hippocampal neurons), NIH3T3 (Very widely used mouse fibroblast cell line; 3T3 cells have been derived from different mouse strains and it is therefore important to define the particular cell line. NIH strain were from the National Institute of Health in the USA), and N18 (Mouse neuroblastoma cells) respectively. The data has been normalized to the activity of the pGL3-Promoter vector. Luciferase activity is lost in all cell lines at +33 bp.

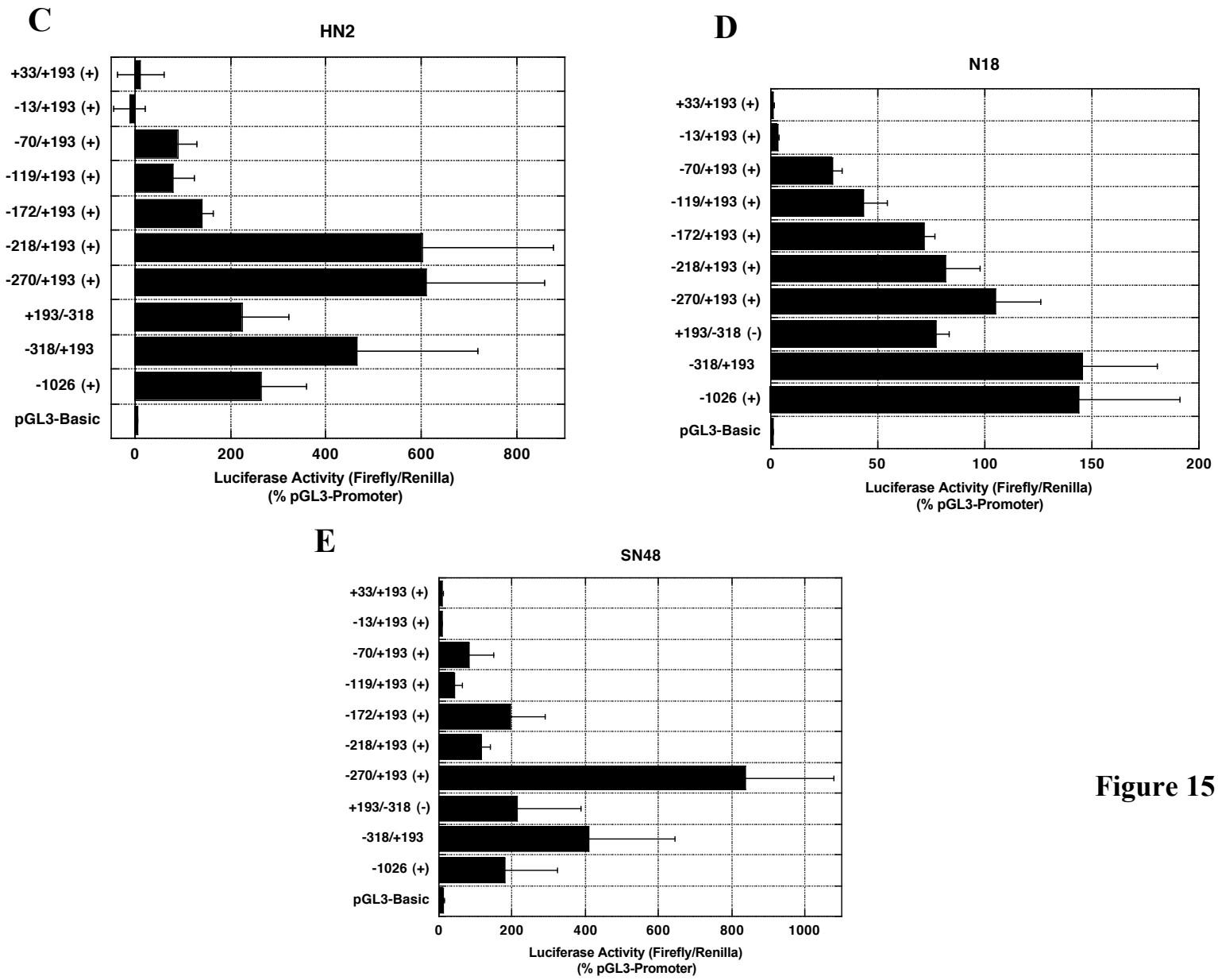

Figure 15 (continued)

Determination of the Possible Transcription Start Site on the Mouse ATPase II Gene by 5' RACE Analysis

The transcription start site of the mouse *ATPase II* gene has not yet been identified. Additionally, the predicted *ATPase II* promoter sequence is devoid of a TATA box or a consensus eukaryotic initiator sequence, and it is known that such TATA-less promoters often contain multiple transcription start sites, which had to be determined. In order to obtain the transcription start site and the complete 5' untranslated sequence of the ATPase II mRNA, the GeneRacer kit (Invitrogen) was used. The RACE kit from Invitrogen, was used in analyzing the human ATPase II promoter.

One important part of this strategy was to design a reverse, gene-specific primer in such a way that genomic DNA contamination could be eliminated from the 5'RACE product. This is achieved by positioning the gene-specific, reverse *ATPase II*-specific primer NM_009727.exon3 and the nested gene-specific reverse primer *ATPase II*-specific primer NM_009727.exon2 **(Table 2c)** on exon 3 and exon 2. As mentioned before, the human ATPase II gene is homologous to the mouse ATPase II gene, we could predict that the 5'untranslated region of the mouse ATPase II gene may also contain many GC-rich regions, as the human ATPase II promoter region [Sobocki 2005]. If this was the case, then PCR amplification of such a template would prove to be a technical challenge. 5'-RACE required two rounds of PCR amplification as described in Materials and methods section. Secondary products were clearly visible upon analysis by agarose gel electrophoresis (Figure 16). The expected size of such secondary products is exactly 30 bp larger due to the presence of an additional stretch of oligodeoxynucleotide originating from a part of the reverse transcribed GeneRacer RNA oligonucleotide sequence at the 5'

ends of the products. We obtained major bands of approximately 350 bp in Heart, Lung, Kidney and Spleen (Figure 15, Table 5). I was unable to obtain any RACE product from brain tissue. The products were cloned into pCR4-TOPO vector and sequenced (total of 4 clones). None of the transcription initiation sites corresponded to the consensus, **YYANT/AYY**, eukaryotic transcription initiation sequence where N was any nucleotide and Y was a pyrimidine nucleotide (Figure 16).

Table 5: Lengths of the 5'RACE products

Tissue	Number of basepairs from Transcription Start (+1) to Translation Start (ATG)
Spleen UB	220 bp
Heart	158 bp
Lung	224 bp
Liver	221 bp

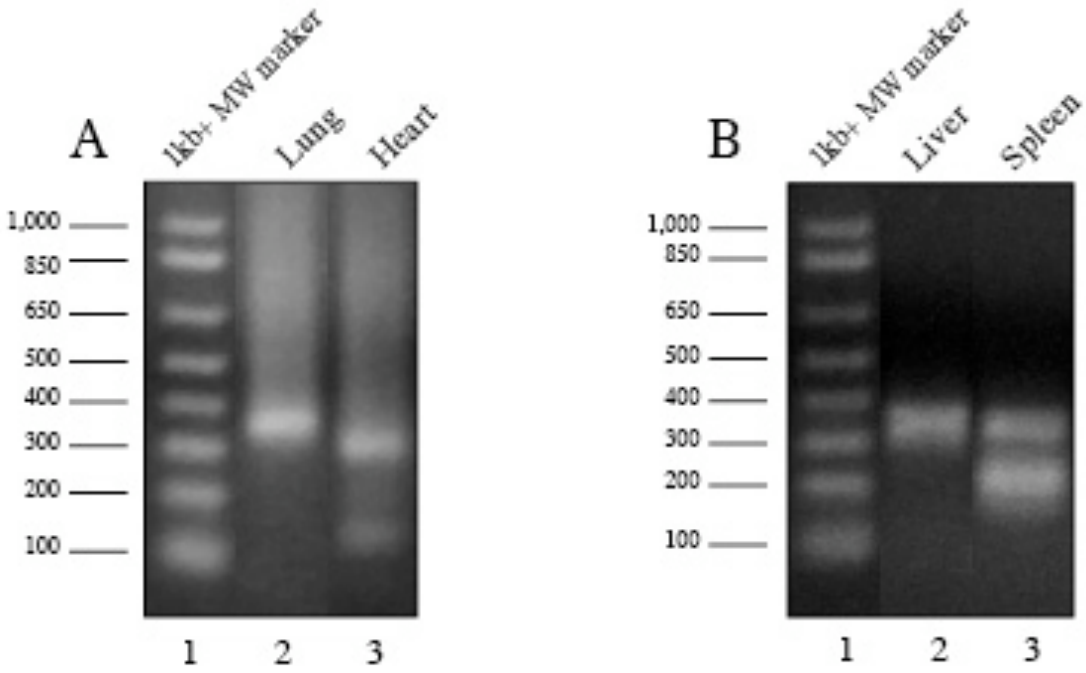

C

```
NM_009727.2   ---ACTGCGG GGAGACCTAG GCGGCTCTGC GGACGCAGCT CCTTCGCCGC CTTCCCCCTC   57
SpleenUB      ----CTGCGG GGAGACCTAG GCGGCTCTGC GGACGCAGCT CCTTCGCCGC CTTCCCCCTC   56
Heart         ---------- ---------- ---------- ---------- ---------- ----------
Lung          CACACTGCGG GGAGACCTAG GCGGCTCTGC GGACGCAGCT CCTTCGCCGC CTTCCCCCTC   60
Liver         ---ACTGCGG GGAGACCTAG GCGGCTCTGC GGACGCAGCT CCTTCGCCGC CTTCCCCCTC   57
```

Figure 16 A-C : RLM-RACE analysis of the *ATPase II* promoter shows that the major transcription start site in the Liver, Heart, Lung and Spleen is ~225-bp 5' of the translation start site. The major band at ~350 bp in all tissues corresponded to transcription start sites at Adenine (+1). Eventhough all the clones were obtained with 5' Reverse Nested Gene-Specific Primer (Table 2c), as a reverse primer, only the 5' part of the sequences of the tissues corresponding to the promoter region indicated is shown in this figure. The location of the coding sequence within the *ATPase II* gene is indicated.

```
NM_009727.2  CCGTCCAGTG CCCAGGCGGC TCCTGGCGGC GACGCTGCCC TGGGTGGGAG GCGCGGCCCC  117
SpleenUB     CCGTCCAGTG CCCAGGCGGC TCCTGGCGGC GACGCTGCCC TGGGTGGGAG GCGCGGCCCC  116
Heart        ------AGTG CCCAGGCGGC TCCTGGCGGC GACGCTGCCC TGGGTGGGAG GCGCGGCCCC   54
Lung         CCGTCCAGTG CCCAGGCGGC TCCTGGCGGC GACGCTGCCC TGGGTGGGAG GCGCGGCCCC  120
Liver        CCGTCCAGTG CCCAGGCGGC TCCTGGCGGC GACGCTGCCC TGGGTGGGAG GCGCGGCCCC  117

NM_009727.2  GCGGCAGCTG AGCCCTCTGC GCGGCGCAGC CAGCTCTCCC GCCCGCGCGG CGCCGTGACA  177
SpleenUB     GCGGCAGCTG AGCCCTCTGC GCGGCGCAGC CAGCTCTCCC GCCTGCGCGG CGCCGTGACA  176
Heart        GCGGCAGCTG AGCCCTCTGC GCGGCGCAGC CAGCTCTCCC GCCCGCGCGG CGCCGTGACA  114
Lung         GCGGCAGCTG AGCCCTCTGC GCGGCGCAGC CAGCTCTCCC GCCCGCGCGG CGCCGTGACA  180
Liver        GCGGCAGCTG AGCCCTCTGC GCGGCGCAGC CAGCTCTCCC GCCCGCGCGG CGCCGTGACA  177

NM_009727.2  GGTGCAGGGT CCCCGCCCGA GACCCACCTG CAGGGGCTGT CGAGATGCCG ACCATGCGGA  237
SpleenUB     GGTGCAGGGT CCCCGCCCGA GACCCACCTG CAGGGGCTGT CGAGATGCCG ACCATGCGGA  236
Heart        GGTGCAGGGT CCCCGCCCGA GACCCACCTG CAGGGGCTGT CGAGATGCCG ACCATGCGGA  174
Lung         GGTGCAGGGT CCCCGCCCGA GACCCACCTG CAGGGGCTGT CGAGATGCCG ACCATGCGGA  240
Liver        GGTGCAGGGT CCCCGCCCGA GACCCACCTG CAGGGGCTGT CGAGATGCCG ACCATGCGGA  237

NM_009727.2  GGACAGTGTC GGAGATCCGC TCGCGCGCGG AAGGTTATGA GAAGACAGAT GATGTTTCAG  297
SpleenUB     GGACAGTGTC GGAGATCCGC TCGCGCGCGG AAGGTTATGA GAAGACAGAT GATGTTTCAG  296
Heart        GGACAGTGTC GGAGATCCGC TCGCGCGCGG AAGGTTATGA GAAGACAGAT GATGTTTCAG  234
Lung         GGACAGTGTC GGAGATCCGC TCGCGCGCGG AAGGTTATGA GAAGACAGAT GATGTTTCAG  300
Liver        GGACAGTGTC GGAGATCCGC TCGCGCGCGG AAGGTTATGA GAAGACAGAT GATGTTTCAG  297

NM_009727.2  AGAAGACCTC GCT                                                    310
SpleenUB     AGAAGACCTC GCT                                                    309
Heart        AGAAGACCTC GCT                                                    247
Lung         AGAAGACCTC GCT                                                    313
Liver        AGAAGACCTC GCT                                                    310
```

Organization of ATPase II Gene:

Alignment of the ATPase II cDNAs with the mouse genome sequence revealed that the *ATPase II* gene was located on chromosome 5qC3.1 and spanned the region from base 66, 388,741 to base 66,614,924 with the coding sequence matching with the negative strand between bases 66,614, 926 and 66,388,741 within chromosome 5. The gene was composed of 36 exons (sizes: 41 to 184 bp) and 37 introns. The exon/intron organization is shown in **Table 6**.

Table 6: Exon-Intron Boundaries of the Mosue *ATPase II* Gene

Exon	cDNA NM_001038999.1		cDNA NM_009727.2		Exon Size (bp)	Chromosome 5		IntronExonIntron
	From	To	From	To		From	To	
1	1	270	1	270	270	67204522	67204253	……..CGGAAG|gtgagt
2	271	385	271	385	115	67168495	67168381	tttcag|GTTATG……..CGTCAG|gtagga
3	386	485	386	485	100	67166963	67166864	ttccag|TACTGC…….CTCCAG|gtaaag
4	486	584	486	584	99	67165958	67165860	tttcag|CAAATT…….GATATT|gtaagt
5	585	630	585	630	46	67159474	67159429	ctttag|AAACGA…….CACAAG|gtagga
6	631	671	631	671	41	67142183	67142143	ctgcag|TTTTGA…….GAAAAG|gtatgt
7	-	-	672	745	74	67136595	67136522	tttcag|GTAAAT…….GTCAAG|gtagag
8	672	745	-	-	74	67134567	67134494	gtgtag|GTGGCA……..CTCAAG|gtcaga
9	746	815	746	815	70	67131751	67131682	caacag|TGAGCC…….AGACAA|gtaagt
10	816	943	816	943	128	67130403	67130276	caacag|GGCTTA…….CCATGG|gtatgt
11	944	1055	944	1055	112	67124716	67124605	tcctag|CACCGT…….ATGCAG|gtgaga
12	1056	1221	1056	1221	166	67122738	67122573	ttacag|AATTCC……..TACACT|gtgagc
13	1222	1349	1222	1349	128	67120514	67120387	caacag|ATGGTG……..AATTGG|gtaaat
14	1350	1427	1350	1427	78	67118116	67118039	ttgtag|GATCTT……..GGCCAG|gtaagc
15	1428	1516	1428	1516	89	67116725	67116637	ttgcag|GTTAAA…….CTATGG|gtgagc
16	1517	1561	-	-	45	67112217	67112173	ctgaag|CCATGT……..TGAATG|gtaagc
17	1562	1634	1517	1589	73	67106608	67106536	ctttag|GCAGAG……..AACCAC|gtaagt
18	1635	1740	1590	1695	106	67104679	67104574	tcacag|CCAACC…….CGCCAG|gtacac
19	1741	1823	1696	1778	83	67102883	67102801	tcacag|ATGAGG……..GATTCA|gtaagt
20	1824	1873	1779	1828	50	67101152	67101103	ctgcag|CTGGGG…….CACCAG|gtaaag
21	1874	1943	1829	1898	70	67094005	67093936	tttcag|TGCTAG…….GGAGCT|gtaagt
22	1944	2028	1899	1983	85	67087776	67087692	ttccag|GACACA…….CAGAAG|gtgagc
23	2029	2168	1984	2123	140	67085454	67085315	ttacag|GGCTGA……..GAAAAG|gtgcgt
24	2169	2307	2124	2262	139	67061567	67061429	ccccag|AATCTT…….ATATTG|gtaatt
25	2308	2372	2263	2327	65	67058567	67058503	ccccag|GACACT……..CTTGAC|gtaagt
26	2373	2545	2328	2500	173	67038453	67038281	ttccag|GGCACG……..CTGCAG|gtaagt
27	2546	2729	2501	2684	184	67023230	67023047	tccaag|GGTTTC……..GCTCAG|gtaaag
28	2730	2840	2685	2795	111	67022954	67022844	ccatag|TTCAAA…….ATCGAG|gtagcc

Table 4 (Continued) – Exon Intron Boundaries of the Mouse *ATPase II* Gene

33	3180	3236	3135	3191	57	67004104	67004048	ttttag|TTTGTA…….ACATGG|gtaaga
34	3237	3344	3192	3299	108	67003323	67003216	ccgcag|TTCAGC…….GGAGAG|gtaatg
35	3345	3433	3300	3388	89	66987098	66987010	tcgcag|GCAGCC…….CAAAGT|gtgagt
36	3434	3526	3389	3481	93	66986306	66986214	ccacag|CATCAA……..AAAGAG|gtaaaa
37	3527	3618	3482	3573	92	66979624	66979533	ccacag|CCTCAC…….TGCTTC|gtgagt

Chapter 4

Discussion:

The P-type ATPase superfamily is an evolutionarily conserved, large family of proteins members of which are widely expressed in both prokaryotes and eukaryotes, including bacteria, yeast, parasites, nematodes, insects, plants, and animals [Review, Paulusma 2005]. Many P-type ATPases and their coding sequences have been identified. These ATPases are integral membrane proteins, which in most cases, mediate the ATP-dependent transport of small cations across biological membranes, including those of intracellular organelles. The type 4 subfamily constitutes a relatively new branch of the phylogenetic tree of P-type ATPases and as mentioned previously they are putative aminophospholipid translocases (APTL). The idea that mammalian members of this subfamily have a role in the translocation of (amino)-phospholipids is mainly based on the characterization of their yeast homologs. The biochemical activity and the substrate specificity of most of these mammalian proteins remain to be elucidated. Ding et al was the first group to demonstrate a convincing correlation between biochemical activity and substrate specificity of mammalian ATPase II (ATP8A1) [Ding 2002]. After purification of 4 bovine ATPase II isoforms and subsequent reconstitution into a defined lipid environment, these researchers demonstrated an aminophospholipid (PS and PE)-specific activation of the ATPase activity of these proteins, strongly suggesting that ATP8A1 is indeed an aminophospholipid translocase [Ding 2002].

Based on these findings, our study was focused on determining whether or not the mouse ATPase II homolog of Drs2p has an APTL activity. Although some of the ATPase

genes are believed to be putative aminophospholipid translocases (APTL), our studies have shown that overexpression of the mouse cDNA for such a P-type ATPase (the *ATPase II* cDNA) in the mouse hippocampal neuron-derived cell line HN2 causes an increase in aminophospholipid translocase activity (Figure 3 & 4). These results confirm that this ATPase II has an aminophospholipid translocase activity or could be involved in regulating the function of APTL.

Previous studies in our lab showed that the overexpression of mouse ATPase II resulted in the unexpected appearance of mixed, voltage-gated calcium currents in the normally calcium current-deficient HN2 cells [Chin 2003]. The possible reasons for the appearance of mixed calcium current following stable expression of ATPase II could be a result of either induced expression of the calcium channel protein subunits or channel-stimulating protein-protein interactions between ATPase II and calcium channel proteins. The mixed calcium current did not appear in the HN2 cells that were transfected with a heterologous gene placed in the same vector, pCMV6, as used for the expression of ATPase II [Chin 2003]. Also the ATPase II overexpressing clones HN2A12 and HN2A22 express significant levels of the N-type calcium channel core subunit α_{1B}, whereas the HN2 cells show virtually no expression of this protein [Chin 2003]. Aside from the appearance of the N-type calcium current, an L-type component was identified as a result of nifedipine inhibition, (Data not shown).

This observation suggests the possibility that this ATPase II might play an additional role by regulating the expression of other important proteins. This could be the result of stimulation of a signaling cascade by the released phosphate ion, which could then stimulate protein phosphorylation that is important for the APTL activity [Korge

1993, Ramelot 2001, Roach 1976]. An alternate theory could be that the ATPase II molecule directly interacts with other proteins that regulate the expression or activity of the calcium channels. Aside from these theories, we can also hypothesize that the expression of the N-type calcium channel subunit could be due to the activation of ERK which resulted in the induction of the Fos B gene, as illustrated in by Figure 7. It has been shown that most MAPKs (ERKs) phosphorylate transcription factors that are involved in the induction of *fos* genes, whose products heterodimerize with Jun proteins to form the activation protein-1 (AP-1) complexes [Chang 2001]. It so happens that the promoter of the N-type calcium channel subunit α_{1B} and the promoter of the L-type calcium channel subunit α_{1C} habor many AP-1 binding sites, which leads us to speculate that perhaps the activation of MAPK which results in the binding of the phosphorylated heterodimers cJun/cFos to the AP-1 sites present on the promoter of the calcium channel core subunit α_{1B} [Fan 2002, Kim 1997]. This concept is illustrated in Figure 17.

As mentioned before, changes in the concentration of the intracellular as well as the extracellular calcium levels cause an inhibition of both the ATPase and phospholipids-translocase activity of APTL [Zwaal 1997]. Many studies have emphasized the central role of the calcium ion in the regulation of cell death. Calcium can activate distinct parts of the cell death program, which can then function alone or in conjunction with other sub-programs to kill the cell. Recent findings have provided evidence for crosstalk between calpains, caspases and other protease families, and have indicated new pathways that lead directly from a calcium signal to caspase activation and apoptosis [Orrenius 2003]. However, the analysis of the role of ATPase II during apoptosis showed that stress did not have any significant effect on the activity of APTL

in the ATPase II overexpressing cells, which exerts a check on the proapoptotic enzyme caspase-3, and also activation of the mitogen-activated protein kinases Erk1/2, which regulate gene expression and apoptosis (Figures 5,6, & 7). This observation contradicts our findings versus the findings of many other researchers involving the role of calcium in apoptosis. Recent studies in support of our findings have shown that following activity deprivation and reduced entry of calcium ions through voltage dependent calcium channels (VDCC), activated cyclin B/CDC 2 catalyzes the phosphorylation of the BH3-only protein Bad at Ser-128, which lies near the growth factor regulated site of phosphorylation, Ser-136. The CDC2 induced phosphorylation of Bad at Ser-128 inhibits the ability of 14-3-3 proteins to sequester Ser-136 phosphorylated Bad and thereby promote the apoptotic effect of Bad [Becker 2004]. Therefore we can hypothesize that the voltage gated calcium channels that unexpectedly appeared as a result of ATPase II overexpression, could reverse the effect by causing a moderate, but not excitotoxic increase in Ca^{2+} entry through N- and L-type channels thereby preventing apoptosis via inhibition of caspase-3 activity as illustrated by Figure 17.

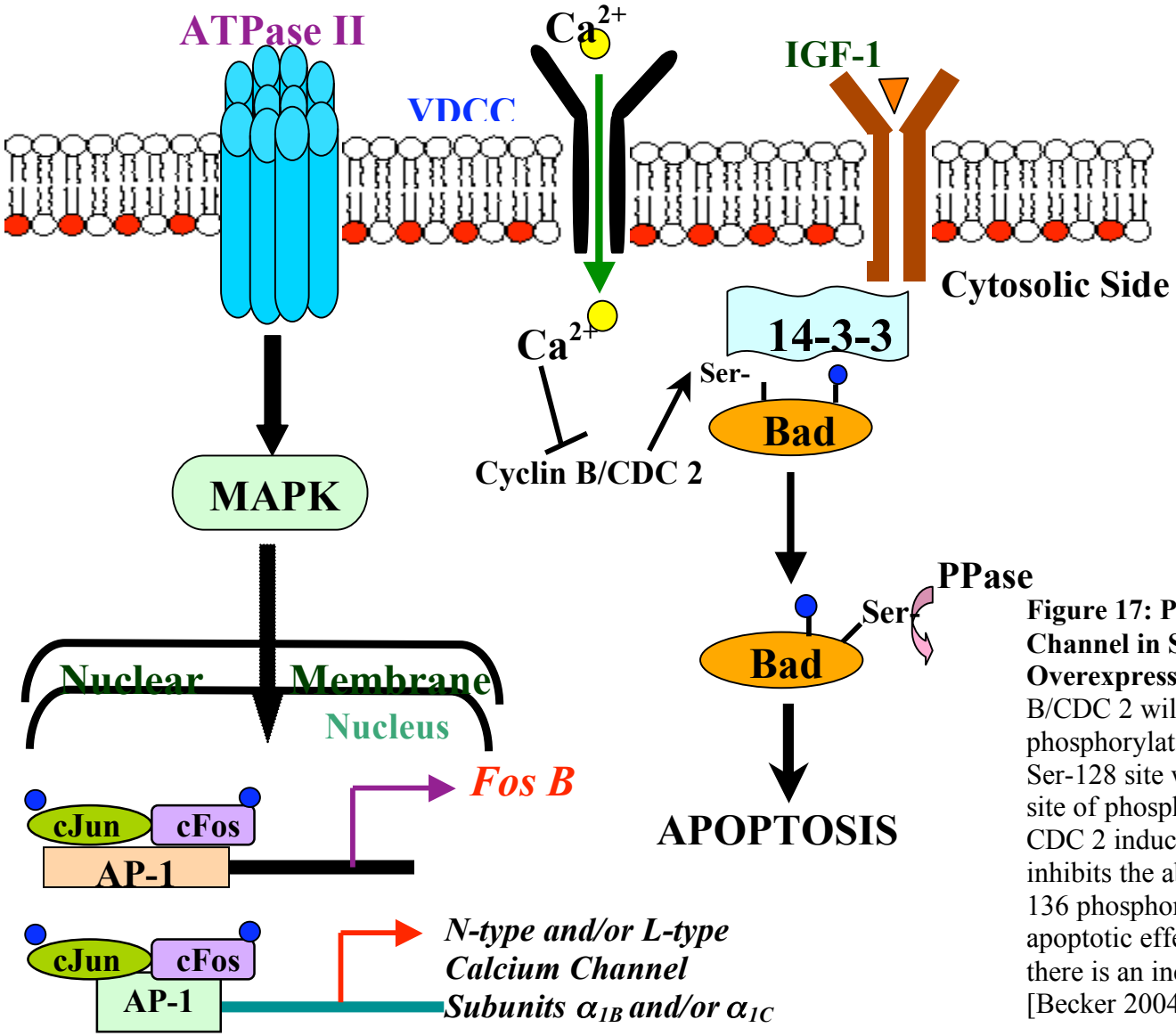

Figure 17: Possible Role of Voltage Gated Calcium Channel in Signaling Cascade due to ATPase II Overexpression. If calcium enters via VDCC, cyclin B/CDC 2 will get inactivated therefore phosphorylation of the "BH3-Only" protein Bad at the Ser-128 site which is near the growth factor regulated site of phosphorylation Ser-136 will not occur. The CDC 2 induced phosphorylation of Bad at Ser 128 inhibits the ability of 14-3-3 proteins to sequester Ser-136 phosphorylated Bad and therefore promotes the apoptotic effect of Bad. This effect is reversed when there is an increase in calcium entry via VDCC [Becker 2004}.

One of the many objectives of this study was to prove that ATPase II harbor APTL activities. Previous, studies have shown that in yeast that an ATPase II mutant, a product of the DRS2 gene, showed a deficiency in the uptake of PS, which led to a preliminary conclusion that ATPase II showed APTL activity. Results from other assays however have proven that this deficiency was not specific with other drs2 mutants [Mouro 1999]. A series of assays were conducted in order to prove that ATPase II was specific to APTL activity (Figure 4).

Following the standardization of the dithionite-based 96-well assay, APTL activity was mentioned in B16F10 and HN2 cells transfected with mATPase II expressing vectors. It can be seen clearly in Figure 8, that the over-expressing clones showed a significant increase in APTL activity, which leads us to further believe that ATPase II is a protein that contributes to the function of APTL.

If indeed this ATPase II is central to the inner membrane localization of PS and is responsible of APTL like activity, then inhibition of the function of ATPase II or a decrease in the expression of this enzyme would result in the externalization of PS. This hypothesis was confirmed when transient transfection of full-length, antisense ATPase II cDNA caused PS externalization, as shown in Figure 9. In order to further verify the correlation between APTL activity for ATPase II that was seen in Figures 4 and 8, B16F10 cells were transfected with the antisense vector of ATPase II. Figure 10 shows the expected results of significantly decreased APTL activity when this construct was transfected into B16F10 cells, thereby validating that ATPase II does contribute significantly to APTL function. However, it cannot be concluded that ATPase II is solely

responsible for the internalization of PS, because there is still some residual APTL activity in the cells.

Previous studies have shown that the expression profile of ATPase II vary in different cell and tissue types [Halleck 1998, Halleck 1999]. Based on these observations, we planned to investigate the structure and role of the *ATPase II* promoter. The mouse is an effective model system, which has been used by many research groups to understand targeted genetic alterations that closely resemble many human diseases. Therefore elucidation of the mouse promoter is an important task because this could lead to the understanding of the observed tissue-specific expression of ATPase II. As described previously Chin *et al*, the appearance of mixed calcium current following the overexpression of ATPase II was observed in a mouse cell line (HN2) [Chin 2003]. In addition to this observation, the tissue-specific regulation of ATPase II transcripts was first observed in the mouse model and in the human model. Based on our observations and previous studies, we decided to isolate and analyze the mouse ATPase II promoter using the same approach that was used in the isolation of the human ATPase II promoter [Sobocki 2005]. We have seen some sequence homology between the mouse and human ATPase II sequence. The predicted core promoter runs from nucleotide 742 to 1252.

As discussed earlier, the *ATPase II* promoter lacks a TATA box and contain GC-rich regions harboring multiple transcription factor binding sites, Tables 3 & 4. The promoter region of the *ATPase II* gene is located upstream (~ 350 bp) from the translation-start site of the *ATPase II* gene, as illustrated by Figure 11. Deletion analysis of the *ATPase II* promoter indicated the possible presence of repressor and/or enhancer elements which varied from cell-line to cell-line (Figures 12 & 15). Repressor elements

could still be present in the promoter either upstream or downstream of the ~1.2 kb sequence that was analyzed in this study, as can be clearly seen by the decrease or lack their of luciferase reporter activity in the distal promoter (Figure 12).

The mouse and human promoter have many of the important transcription factors such as – NFKappa B, SP1 (stimulating protein), AP2 (activating protein 2), AP4 (activating protein 4) and the CPBP (core promoter binding protein). These transcription factors have their unique functions and role in a tissue or cell-type specific manner, as described in Table 3. For example, the transcription factor SP1 is a protein present in mammalian cells that bind to the GC box promoter elements and selectively activates mRNA synthesis from genes that contain functional recognition sites [Mermod 1988]. This further indicates that the GC-rich region of the promoter is indeed the core promoter, as illustrated by Figure 13 & 14. In addition to SP1, studies have shown that interaction of both p50 and p65 subunits of the heterodimeric NF-Kappa B complex with DNA is required for DNA binding and transcriptional activation [Williams 1991]. The p50 and p65 subunits play a role in cell cycle regulation. The AP-4 transcription factor is an enhancer-binding factor, which activates SV40 (simian virus) late transcription in vitro [Koritschoner 1997]. Then the mammalian transcription factor AP-2 is a retinoic acid inducible sequence specific DNA-binding protein that is developmentally regulated [Koritschoner 1997]. Finally, the core promoter-binding protein (CPBP) is an essential element of a TATA less promoter. The tissue distribution of CPBP mRNA revealed that it is differentially expressed with an apparent enrichment in placental cells [Koritschoner 1997]. The DNA binding and transcriptional activity of CPBP, in conjunction with its expression pattern, strongly suggests that this protein may participate in the regulation

and/or maintenance of other TATA box-less genes [Koritschoner 1997]. The functional role of the transcription factors present in both mouse and human putative ATPase II promoter, suggests that the promoters are TATA-less.

Despite the similarities, the mouse promoter also has a few different binding sites for transcription factors such as – AT rich sequence binding protein, the Egr-2/Krox-20 early growth response gene product and the cAMP responsive element binding (CREB) protein. The special AT-rich sequence-binding protein 1, is a cell type-specific nuclear matrix attachment region (MAR) DNA-binding protein, predominantly expressed in thymocytes [Dickinson 1997]. Egr2 is a nerve growth factor induced protein C, this is a zinc finger transcription factor [Dickinson 1997]. Finally, the ubiquitous transcriptional factor CREB forms a ternary complex with the human T-cell lymphotropic virus type I (HTLV-1) transactivator, Tax, and the 21-bp repeats in the HTLV-I transcriptional enhancer [Dickinson 1997]. The presence of the different transcription factor binding sites indicates the cell-type specificity of the ATPase II promoter in human and mouse could be different.

The overall activity of both the full and core promoters of this gene show similar activity and the deletions of the core promoter showed a sharp yet varying decrease in the activity between -318/-172 in all five different cell lines (Figure 15). This region harbors the following transcription factors, SP1, AP1 and CPBP, and many others as described in Table 3 and 4, which maybe important in the activity of the *ATPase II* promoter in all of the above tested cell lines. For example, fragment -270 showed a higher luciferase reporter activity than both the sense and anti-sense oriented core promoter fragments, however at fragment -218 the luciferase activity drops, and this fragment lacks the

following transcription factors – ZID, CP2 and NFKappaB50, as illustrated by Figure 15 & Table 3. From this point the next few fragments -119 through +33, the luciferase reporter activity starts decreasing down to 7 fold almost to the level of the pGL3 basic empty vector. Luciferase activity is higher in fragment -172 in both B16F10 and NIH3T3 (both non-neuronal) cell-lines compared to the three neuronal cell-lines, where the drop in promoter activity is seen starting at fragment -172, Figure 15. Additionally, NIH3T3 shows a similar profile as B16F10, except for the luciferase activity in fragment -119 which is higher compared to that in B16F10 and all the other neuronal cell-lines. Therefore, we could speculate that NIH3T3 could be expressing the transcription factors that the other cell-lines are not expressing. Since transcription factors are proteins, the expression profile of these proteins can vary from cell-line to cell-line and tissue to tissue, which could confirm our observation of varying profiles of luciferase activity from cell line to cell line. Further characterization of this promoter and the specificity of the transcription factors should be studied. Additionally, the variation in luciferase reporter activity of this promoter could be an indicative of the importance of this ATPase II gene from cell to cell and tissue to tissue.

Aside from analyzing the deletion fragments of the core promoter, we studied the activity of the core promoter in both orientations (sense and anti-sense). It has been known for many years that individual examples of bidirectional genes pairs and in some cases bidirectional promoters regulate the transcription of a gene pair whose levels need to be coordinately expressed for various reasons [Trinklein 2004]. For example, some bidirectional promoters serve to maintain a stoichiometric relationship, such as histone genes, whereas others regulate the coexpression of genes that function in the same

biological pathway, or to control expression through different timepoints such as genes involved in the cell cycle [Trinklein 2004]. Other bidirectional promoters provide coordinated responses to induction signals such as heat shock. Many groups have noted that GC-rich promoters function in both directions. Since our promoter is a TATA-less and has a high GC content, we tested the effect of the luciferase reporter activity by studying the core promoter in a bidirectional manner, with the exception of the B16F10 cell-line, all the other cells had a higher to almost same (SN48) luciferase reporter activity in the sense oriented core fragment versus the anti-sense oriented core fragment, as illustrated by Figure 15.

This tissue specificity was also confirmed when 5' RACE analysis of the mouse *ATPase II* gene was studied, where the size of the transcript varied in size in heart versus the other three tissue types analyzed. We determined the transcription start site to be the "G" based on two independently sequenced clones for the lung tissue, which also had a longer transcript compared to the other tissue types, as illustrated by Figure 16. This varying size in transcript could indicate the rapid need for this protein.

Previous studies on the *ATPase II* gene have reported its cDNA sequences from bovine, mouse and human [Halleck 1999, Mouro 1999, Tang 1996]. However, the intron-exon organization of this gene has not been delineated in these papers. Our analysis of the mouse *ATPase II* gene has yielded the complete organization of the gene at the locus 5qC3.1 on the mouse genome (Table 6). *ATPase II* appears to be a large gene with 36 exons and 37 introns (Table 6).

It has been reported that this gene is highly expressed in the brain [Halleck 1998, Halleck 1999]. Our expectations, is that the *ATPase II* promoter is neuron-cell specific,

our data has shown that this promoter may have some dramatic cell type-specificity [Sobocki 2005]. The P-type ATPases have received a lot of attention in recent years. The involvement of these proteins in Wilson's disease and familial Cholestasis has been established in many studies. The genes for such physiologically important proteins often undergo regulated expression to help maintain appropriate levels of the gene products. Moreover, during apoptosis, many other genes and their products are regulated to effect signature changes that are observed in apoptotic cells. As illustrated before in Figures 3, 4 & 8, the overexpression of ATPase II in the hybrid neuroblastoma cell line HN2 causes an increase in APTL activity. Our earlier studies have also shown that apoptosis is associated with an inhibition of APTL and externalization of PS [Adayev 1998, Das 2003]. Because of this correlation, it could be expected that ATPase II could be linked to the expression and regulation of apoptosis-associated proteins. Thus, there is a need for a thorough analysis of ATPase II expression in various cell types under different conditions of trophic support or stress.

From the results presented in this study, it can be seen that ATPase II expression levels have clear association with APTL activity and function. The next step in this process of proving the connection between these ATPases and APTL would be to knockdown the expression of ATPase II in hopes of ablating both the expression of ATPase II specifically and its function (APTL activity). This would validate the specificity of ATPase II to the translocation of PS to the inner leaflet of the cell membrane. If this is proven successfully, then ATPase II expression can be ablated in cancerous cells in hopes of decreasing APTL activity to effect PS externalization to the outer leaflet of the cell membrane, thereby triggering phagocytosis of these harmful cells.

References:

Adayev, T., Estephan, R., Meserole, S., Mazza, B., Yurkow, E.J., and Banerjee, P. (1998) *Externalization of phosphatidylserine may not be an early signal of apoptosis in neuronal cells, but only the phosphatidylserine-displaying apoptotic cells are phagocytosed by microglia.* J.Neurochem. **71:** p. 1854-1864

Becker, E.B.E, Bonni, A. (2004) *Cell Cycle Regulation of Neuronal Apoptosis in Development and Disease*. Progress in Neurobiology. **72:** p. 1-25

Benimetskaya, L., Miller, P., Benimetsky, S., Maciaszek, A., Guga, P., Beaucage, S.L., Wilk, A., Grajkowski, A., Halperin, A.L., and Stein, C.A. (2001) *Inhibition of potentially anti-apoptotic proteins by antisense protein kinase C-alpha (Isis 3521) and antisense bcl-2 (G3139) phosphorothiate oligodeoxynucleotides: relationship to the decreased viability of T24 bladder and PC3 prostate cancer cells.* Mol. Pharmacol. **60**: p. 1296-1307

Birnbaumer, L., Campbell, K.P., Catterall, W.A., Harpold, M.M., Hoffmann, F., Horne, W.A., Mori, Y., Schwartz, A., Snutch, A., Tanabe, T., Tsien, R.W. (1994) *The Naming of Voltage-Gated Calcium Channels.* Neuron. **13:** p. 505-506.

Bratton, D.L., Fadok, V.A., Richter, D.A., Kailey, J.M., Guthrie, L.A., and Henson, P.M. (1997) *Appearance of phosphatidylserine on apoptotic cells requires calcium-mediated non-specific flip-flop and is enhanced by loss of the aminophospholipid translocase.* J. Biol. Chem. **272**: p. 26159-26165.

Bull, L.N., van Eijk, M.J.T., Pawlikowska, L., DeYoung, J.A., Juijn, J.A., Liao, M., Klomp, L.W.J., Lomri, N., Berger, R., Scharschmidt, B.F., Knisely, A.S., Houwen, R.H.J., and Freimer, N.B. (1998) *A Gene Encoding a P-Type ATPase Mutated in Two Forms of Hereditary Cholestasis.* Nature Genetics. **18:** p. 219-224

Chang, L., Karin, M. (2001) *Mammalian MAP Kinase Signalling Cascades*. Nature. **410:** p. 37-40.

Chin, G., El-Sherif, Y., Jayman, F., Estephan, R, Wieraszko, A., and Banerjee, P. (2003) *Overexpression of Aminophospholipide Translocase cDNA in Neuronal HN2 Cells Causes Appearance of N-type Calcium Channels.* Brain Research. **117:** p.109-115.

Daleke, D., and Lyles, J. (2000) *Identification and Purification of Aminophospholipid Flippases.* Biochim.Biophys.Acta. **1486:** p. 108-127.

Das, P., Estephan, R., and Banerjee, P. (2003) *Apoptosis is associated with an inhibition of aminophospholipid translocase (APTL) in CNS-derived HN2-5 and HOG cells and phosphatidylserine is a recognition molecule in microglial uptake of the apoptotic HN2-5 cells.* Life Sci. **72**: p. 2617-2627.

Deveraux, Q.L., Takahashi, R., Salvesen, G., and Reed, J.C. *X-Linked IAP is a Direct Inhibitor of Cell-Death Proteases.* Nature. **388:** p. 300 - 304

Dickinson, L.A., Dickinson, C.D., and Kohwi-Shigematsu, T. (1997) *An atypical homeodomain in SATB1 promotes specific recognition of the key structural element in a matrix attachment region.* J. Biol. Chem. **272:** p. 11463-11470

Ding, J., Wu, Z., Crider, B.P., Ma, X.L., Slaughter, C., Gong, L., and Xie, X.S. (2000) *Identification and Functional Expression of Four Isoforms of ATPase II, the Putative Aminophospholipid Translocase.* J. Biol. Chem. **275:** p. 23378-23386.

Duvall, E., Wyllie, A.H., and Morris, R.G. (1985) *Macrophages Recognition of Cells Undergoing Programmed Cell Death (Apoptosis).* Immunology. **56:** p. 351

Fadeel, B., Gleiss, B., Högstrand, K., Chandra, J., Wiedmer, T., Sims, P.J., Henter, J., Orrenius, S., and Samali, A. (1999) *Phophatidylserine Exposure During Apoptosis Is a Cell-Type Specific Event and Does Not Correlate with Plasma Membrane Phospholipid Scramblase Expression*. Biochem. Biophys. Res. Commun. **266:** p. 504-511

Fadok, V.A., Savil, J.S., Haslett, C., Bratton, D.L., Doherty, D.E., Campbell, P.A., and Henson, P.M. (1992) *Different Populations of Macrophages Use Either The Vitrnectin Receptor or The PhosphatidylSerine Receptor To Recognize and Remove Apoptotic Cells.* The Journal of Immunology. **149**: p.4029-4035

Fan, Q.I., Vanderpool, K., Marsh, J.D., (2002) *A 27 bp Cis-Acting Sequence is Essential for L-type Calcium Channel α_{1C} Subunit Expression in Vascular Smooth Muscle Cells*. Biochim. Biophys. Acta **1577:** p. 401-411.

Gleiss, B., Gogvadze, V., Orrenius, S., and Fadeel, B. (2002) *Fas-triggered phosphatidylserine exposure is modulated by intracellular ATP.* FEBS Lett. **519**: p. 153-158.

Glondu, M., Liaudet-Coopman, E., Derocq, D., Platet, N., Rochefort, H., and Garcia, M. (2002) *Down-regulation of cathepsin-D expression by antisense gene transfer inhibits tumor growth and experimental lung metastasis of human breast cancer cells.* Oncogene. **21**: p. 5127-5134.

Halleck, M.S., Pradhan, D., Blackman, C., Berkers, C., Williamson, P., and Schlegel, R.A. (1998) *Multiple Members of a Third Subfamily of P-Type ATPases Identified by Genomic Sequences and ESTs.* J. Genome Research. p.354-361

Halleck, M.S., Pradhan, D., Blackman, C., Berkes, C., Williamson, P., and Schlegel, R.A. (1999) *Differential Expression of Putative Transbilayer Amphipath Transporters.* Physiol. Genomics. p.139-150

Hanada, K., and Pagano, R.E. (1995) *A Chinese Hamster Ovary Cell Mutant Defective in The Non-endocytic Uptake of Fluorescent Analogs of Phosphatidylserine: Isolation Using a Cytosol Acidification Protocol.* J. Cell. Biol. **128:** p.793-804

Kadonaga, J.T., Carner , K.R., Masiarz, F.R., and Tjian, R. (1987) *Isolation of cDNA Encoding Transcription Factor Sp1 and Functional Analysis of the DNA binding domain.* Cell. **51:** p. 1079-1090

Kent, W.J. (2002) BLAT – The BLAST-like alignment tool, Genome Res. **12:** p. 656-664.

Kent, W.J., Sugnet, C.W., Furey, T.S., Roskin, K.M., Pringle, T.H., Zahler, A.M. (2002) *The Mouse Genome Browser at UCSC.* Genome Res. **12:** p. 996-1006

Kim, D.S., Jung, H.H., Park, S.H., Chin, H. (1997) *Isolation and Characterization of the 5'-Upstream Region of the Human N-type Calcium Channel α_{1B} Subunit Gene*. The Journal of Biol. Chem. **272:** p. 5098-5104.

Koritschoner, N.P., Bocco, J.L., Panzetta-Dutari, G.M., Dumur, C.I., Flury, A., Patrito, L.C. (1997) *A novel human zinc finger protein that interacts with the core promoter binding element of a TATA box-less gene*. J. Biol. Chem. **272:** p. 9573-9580

Kunsch, C., Ruben, S.M., and Rosen, C.A. (1992) *Selection of optimal kappaB/Rel DNA-binding motifs: interaction of both subunits of NF-KappaB with DNA is required for transcriptional activation*. Mol. Cell. Biol.

Kühlbrandt, W. (2004) *Biology, Structure and Mechanism of P-type ATPases*. Nature Reviews – Molecular Cell Biology. **5:** p. 282-294

Laplante, J.M., O'Rourke, F., Lu, X., Fein, A., Olsen, A., and Feinstein, M.B. (2000) *Cloning of human Ca^{2+} homoeostasis endoplasmic reticulum protein (CHERP) inhibits intracellular Ca^{2+} mobilization and decreases cell proliferation.* Biochem. J. **348**: p. 189-199.

McIntyer, J.C., Sleight, R.G. (1991) *Fluorescence Assay for Phospholipid Membrane Asymmetry.* Biochemistry. **30:** p. 11819-11827

Mermod, N. Williams, T.J., and Tjian, R. (1988) *Enhancer binding factors AP-4 and AP-1 act in concert to activate SV40 late transcription in vitro.* Nature. **332:** p. 557-561

Miller, R.J. (1992) *Voltage-Sensitive Ca^{2+}Channels.* J. Biol. Chem. **267:** p. 1403-1406.

Mintz, I.M., Adams, M.E., and Bean, B.P. (1992) *P-Type Calcium Channels in Rat Central and Peripheral Neurons.* Neuron, **9:** p.85-89.

Morrot, G., Herve, P., Zachowski, A., Fellmann, P., and Devaux, P.F. (1989) *Aminophospholipid Translocase of Human Erythrocytes: Phospholipid Substrate Specificity and Effect of Choleterol.* Biochemistry. **28:** p. 3456-3462

Mouro, I., Halleck, M.S., Schlegel, R.A., Genevieve, M.M., Williamson, P., Zachowski, A., Devaux, P., Cartron, J., and Colin, Y. (1999) *Cloning, Expression, and Chromosomal Mapping of a Human ATPase 2 Gene, Member of the Third Subfamily of P-Type ATPases and Orthologous to the Presumed Bovine and Murine Aminophospholipid Translocase*. J. Biol. Chem. **257:** p. 333-339

Myers, K.J., and Dean, N.M. (2000) *Sensible use of antisense: how to use oligonucleotides as research tools.* TiPS. **21**: p. 19-23.

Novina, C.D., Roy, A.L. (1996) *Core Promoters and Transcriptional Control.* Trends Genetics. **12:** p. 351-355

Orrenius, S., Zhivotovsky, B., Nicotera, P. (2003) *Regulation of Cell Death: The Calcium-Apoptosis Link.* Nature Reviews – Molecular Cell Biology. **4:** p. 552-565

Paulusma, C.C., Elferink, R.P.J.O. (2005) *The Type 4 Subfamily of P-Type ATPases, Putative Aminophospholipid Translocases with a Role in Human Disease.* Biochim. Biophys. Acta. **1741:** p. 11-24.

Pomorski, T., Hermann, A., Zimmermann, B., Zachowski, A., Muller, P. (1995) *An Improved Assay for Measuring the Transverse Redistribution of Fluorescent Phospholipids in Plasma Membranes.* Chemsitry and Physics of LPIDS. **77:** p. 139-146
Porat, Y., Kolusheva, S., Jelinek, R., Gazit, E. (2003) *The Human Islet Amyloid Polypeptide Forms Transient Membrane-Active Prefibrillar Assemblies.* Biochemistry

Quandt, K., Frech, K., Karas, H., Wingender, E., Werner, T. (1995) *MatInd and MatInspector: New Fast and Versatile Tools for Detection of Consensus Matches in Nucleotide Sequence Data.* Nucleic Acids Res. **23:** p. 4878-4884

Savill, J., Dransfield, I., Hogg, N., and Haslett, C. (1990) *Vitronectin Receptor-Mediated Phagocytosis of Cells Undergoing Apoptosis.* Nature. **343:** p. 170

Scherf, M., Klingenhoff, A., Werner, T. (2000) *Highly Specific Localization of Promoter Regions in Large Genomic Sequences by PromoterInspector: A Novel context Analysis Approach*. J. Mol. Biol. **297:** p. 599-606

Scott, V.E.S., Waard, M.D., Liu, H., Gurnett, C.A., Venzke, D.P., Lennon, V.A., Campbell, K.P. (1996) *β Subunit Heterogeneity in N-type Ca^{2+} Channels.* J. Biol. Chem. **271:** p. 3207-3212.

Sleight, R.G., Abanto, M.N. (1989) *Differences in Intracellular Transport of a Fluorescent Phosphotidylcholine Analog in Established Cell Lines*. Journal of Cell Science. **93:** p. 363-374

Sobocki, T., Jayman, F., Sobocka, M.B., Duchatellier, R., Banerjee, P. (2005) *Isolation, Sequencing, and Functional Analysis of the TATA-Less Human ATPase II Promoter.* Biochim. Biophys. Acta. **1728:** p. 186-198.

Tang, C.M., Presser, F., Morad, M. (1988) *Amiloride Selectively Blocks the Low Threshold.* Science. **240:** p. 213-215

Tang, X., Halleck, M.S., Schlegel, R.A., and Williamson, P. (1996) *A Subfamily of P-Type ATPases with Aminophospholipid Transporting Activity.* Science. **272:** p. 1495-1497.

Tilly, R.F.A., Senden, J.M.G., Comfurius, P., Bevers, E.M., Zwaal, R.F.A. (1990) *Increased Aminophospholipid Translocase Activity in Human Platelets During Secretions.* Biochim, Biophys. Acta. **1029:** p. 188-190

Trinklein, N.D., Aldred, S.F., Hartman, S.J., Schroeder, D.I., Otillar, R.P., Myers, R.M. (2004) *An abundance of Bidirectional Promoters in the Human Genome*. Genome Research. **14:** p.62-66

Tsivkovskii, R., Eisses, J.F., Kaplan, J.H., Lutsenko, S. (2002) *Functional Properties of the Copper-transporting ATPase ATP7B (the Wilson's Disease Protein) Expressed in Insect Cells.* J. Biol. Chem. **277:** p.976-983

Williams, T., and Tjian, R. (1991) *Characterization of a dimerization motif in AP-2 and its function in heterologous DNA-binding proteins.* Science. **251:** p1067-1071

Zwaal, R.F.A. and Schroit, R.A. (1997) *Pathophysiologic Implications of Membrane Phospholipid Asymmetry in Blood Cells.* Blood. **89:** pp. 1121-1132